Agricultural Water Management 325 (2026) 110184

Contents lists available at ScienceDirect

Agricultural Water Management

journal homepage: www.elsevier.com/locate/agwat

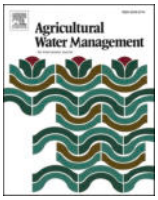

Water and energy savings using variable rate sprinkler irrigation on a large maize farm in northern Italy

Alice Mayer [a,*], Bianca Ortuani [a], Alberto Crema [b], Mirco Boschetti [b], Arianna Facchi [a]

[a] Department of Agricultural and Environmental Sciences (DiSAA), University of Milan, Via Celoria 2, Milano 20133, Italy
[b] Institute for Electromagnetic Sensing of the Environment (IREA), National Research Council of Italy (CNR), Via Bassini 15, Milano 20133, Italy

ARTICLE INFO

Handling Editor - Dr R Thompson

Keywords:
Variable speed control
Homogeneous management unit
Soil moisture sensor
Agro-hydrological model
Weather forecast
Remote sensing

ABSTRACT

Maize is a key crop both globally and in Italy. In the Po Valley, it is cultivated on 500,000 ha, primarily for use in livestock production. Here, maize cultivation is highly dependent on irrigation, traditionally performed using border irrigation. However, due to increasing water scarcity, more efficient irrigation strategies will be required in the future. This study develops and tests an innovative integrated framework combining soil characterisation, in-field monitoring devices, agro-hydrological modelling and remote sensing to save water and energy. In 2021, a variable rate (VR) irrigation strategy was implemented in a 15-ha center pivot in a large livestock farm in northern Italy using: i) soil mapping based on an electromagnetic induction (EMI) sensor to delineate homogeneous zones, ii) a modelling workflow coupling soil moisture probes and weather forecasts to determine irrigation timing and amounts, and iii) a speed-controlled pivot for spatially variable application. This approach reduced water and energy use by 20 %, while maintaining yield and reducing grain moisture at harvest, although operational constraints imposed by the tenant limited the achievable savings. The framework was then scaled up to the entire farm for the 2016–2021 period using a semi-distributed agro-hydrological model supported by remote sensing data. Simulations indicated a mean reduction of 19 % in irrigation and energy use, consistent with field results. Overall, the developed modelling framework proved to be effective in optimizing irrigation and can be transferred to other crop-growing areas relying on sprinkler systems.

1. Introduction

Maize (Zea mays L.) is one of the world's most important and widespread crops, after wheat and rice. Worldwide, it is cultivated on a total area of 203.5 million ha, with a yield of 1.2 million tonnes in 2022 (FAO, n.d.). In Europe, maize is intensively cultivated in France, Italy and Romania. In Italy, although production has fallen slightly in recent years (from 6.1 million tonnes in 2020–5.4 million tonnes in 2023), maize is still one of the most important crops accounting for almost 40 % of total cereal production. In northern Italy, where most of the country's maize production is concentrated, the cultivated maize area reaches approximately 500,000 ha, compared to 4.5 million ha of utilized agricultural land. Here, 30 % of total production is concentrated in four provinces: Turin, Cuneo, Brescia and Mantova (ISTAT, n.d).

The popularity of this crop can be attributed to its versatility. It can be used for human consumption (in the form of cornflakes, bread, maize syrup and oil), for animal feed (due to the high yield and feed value of grains, leaves and stalks) and in the pharmaceutical and industrial sectors (for the production of starch, ethanol, plastics and as a base for the production of antibiotics) (Abd El-Wahed and Ali, 2013). This makes maize cultivation a major contributor to a country's self-sufficiency on several fronts (Greaves and Wang, 2016).

Maize performs best in areas where rainfall is moderately abundant and well distributed throughout the growing season, particularly during the reproductive stages. However, areas with sufficient rainfall and soil water reserves to fully support the high productivity of maize are limited; as a result, maize cultivation in Italy (as in many other geographical areas) relies on irrigation. According to the literature, the seasonal evapotranspiration (ET) of maize under well-watered conditions ranges from less than 500–800 mm (Steduto et al., 2012). Border irrigation is the reference method for maize in many areas, with average application amounts of 100–200 mm (1000–2000 m^3 ha^{-1}) and typically three to four applications per season; areas with a shallow water table may require only one or two applications. In July, at the phenological stage of flowering, daily irrigation use reaches its maximum of 65–75 m^3 ha^{-1}. Approximately half of the crop water requirement is

* Corresponding author.
E-mail address: alice.mayer@unimi.it (A. Mayer).

https://doi.org/10.1016/j.agwat.2026.110184
Received 15 April 2025; Received in revised form 16 January 2026; Accepted 21 January 2026
Available online 24 January 2026

usually supplied by rainfall, while the remainder must be provided through irrigation. Water shortage is most critical between two weeks before and two to three weeks after silking, as stress during this period can reduce growth, delay maturity, and cause biomass and yield losses of up to 50–60 % (Singh and Singh, 1995). Therefore, irrigation must be properly planned throughout the growing season. particularly during this period, to ensure that maize does not suffer from insufficient or excessive irrigation, which would limit its yield.

Border irrigation, which is widely used in the Po Valley, requires high water volumes and generally exhibits low application efficiency (30–60 %; D.d.s, 4346, 2018). Although there are strategies to improve the efficiency of border irrigation (e.g., Masseroni et al., 2022), the common trend in northern Italy, as in many other regions, is to replace surface irrigation systems with pressurized ones, particularly sprinkler systems. Although such a shift aims to increase efficiency and resource use, it must be accompanied by decision-support tools and technologies to ensure effective planning and management of water application.

The need to improve irrigation management is even more urgent if we consider the effects of climate change expected in the coming years in the world, and in particular in the Mediterranean basin (Toreti et al., 2022). Even in the Po Valley basin, a region historically characterised by relatively abundant water resources, climate change is projected to reduce the availability of freshwater for agriculture, while simultaneously increasing the water requirements of crops. A clear example of these evolving climatic conditions was the severe drought that hit the Po Valley in 2022, marked by a significant decline in the Po River‘s water level and a decrease in available irrigation water (Montanari et al., 2023; Xue et al., 2024). In this context of increasing water scarcity and uncertainty, improving the efficiency of on-farm water use becomes a central objective for agricultural sustainability.

Accordingly, driven by the rising costs of agricultural inputs and the growing awareness of the need to conserve natural resources, researchers, agricultural operators and farmers are beginning to consider with interest “Precision Agriculture” (PA) technologies and techniques (Serrano et al., 2020) and in particular Precision Irrigation (PI).

PI involves three main steps. The first is the “precision detection” phase, which aims to monitor the variability of the soil-crop system within fields. It uses various remote or proximal surveying instruments and techniques such as satellites, drones or geophysical sensors to obtain direct or indirect georeferenced measurements of soil properties, crop dynamics (e.g., phenology) and growth (e.g., LAI), topography, yields and product quality at harvest (Matese and Di Gennaro, 2015). From these measurements, variability maps are generated to support the positioning of ground sampling that is often needed to complement the indirect measurements from sensors (Corwin and Scudiero, 2020; Fitzgerald et al., 2006; Fleming et al., 2000; Hedley and Yule, 2009a, 2009b; Nutini et al., 2018; Ortuani et al., 2019; Scudiero et al., 2016).

The next step is the “precision decision” phase. All the maps produced in the previous phase are processed to obtain, through statistical/geostatistical techniques, a map describing the Homogeneous Management Zones (HMZs). This map can be static, if produced once for the whole agricultural season or even for several years (Ali et al., 2022; Breunig et al., 2020; Georgi et al., 2018; Liu et al., 2018; Reyes et al., 2019; Schenatto et al., 2015; Speranza et al., 2023), or dynamic, if it takes into account changes in the cropping pattern change during the growing season (Ali et al., 2023; Cohen et al., 2017; Crema et al., 2020; Evans et al., 2013; Fontanet et al., 2020; Haghverdi et al., 2015; Scudiero et al., 2018; Termin et al., 2023). HMZ maps can be used to create prescription maps for water input dosing (Ahmed et al., 2023; Neupane and Guo, 2019; Thorp, 2020). The most innovative approaches make use of soil moisture probes and/or agro-hydrological models to determine “when” and “how much” to irrigate in each HMZ (Abioye et al., 2020; Adeyemi et al., 2017; Agyeman et al., 2023; Bantchina et al., 2024; Dahal et al., 2020; Flint et al., 2023; Zhang et al., 2021).

Finally, the third step is the “precision actuation” phase, where the irrigation prescriptions are implemented by devices/machines capable of modulating the operational interventions in a variable way. For the irrigation of maize in open field conditions, the most suitable equipment for the application of variable irrigation rates are irrigation machines such as pivots, linear, hippodromes. In recent decades, much progress has been made in the development of modern high-efficiency sprinkler irrigation systems to increase the efficiency of water use for crop production (Feki et al., 2018). These systems, which account for 23 % of the total area covered by irrigation systems worldwide (Serrano et al., 2020), allow a more homogeneous application of water and up to 40 % less volume than traditional gravity methods (Liakos et al., 2017). There are two options for managing water application in a site-specific manner: speed or sector control (Variable Speed Irrigation, VSI), in which the water application is varied in the direction of travel of the sprinkler line by varying its speed, and zone control (Variable Zone Irrigation, VZI), which also allows the irrigation volume to be varied across the direction of travel of the sprinkler line (i.e., along the distribution pipe) through the autonomous control of individual or groups of sprinklers. The cheapest solution is the VSI, as all newer machines can implement this irrigation strategy at no extra cost, and many older machines can be upgraded with a limited investment (Liakos et al., 2017). In the VZI, sprinklers are controlled in groups or sectors, with different water application rates that can be set as a percentage of the standard application rate (typically from 0 % to 200 %). Despite the zero or limited economic investment, these variable rate irrigation strategies are still rarely used. The implementation of VRI requires dedicated technical support for the calibration of the control panels, the processing of prescription maps, and the integration of soil and crop data. However, public or private research and extension services are almost non-existent in Italy. Technical support is often provided by machinery vendors and focuses mainly on installation rather than agronomic optimisation and site-specific management. In this context, demonstration initiatives, such as those funded under the EU Regional Rural Development Programme (RDP), can play a key role in bridging the gap between scientific innovation and agricultural practice by supporting technology dissemination and farmer–researcher interactions.

With the overall aim of proposing precision irrigation solutions for maize that are both environmentally and economically viable for farmers, the specific objectives of this research were as follows. Firstly: to develop and implement a “precision irrigation” approach for a 15-ha centre pivot installed in a large zootechnical farm (300 ha) in northern Italy for the 2021 agricultural season. The approach was based on: i) the characterisation of intra-field soil variability using a geophysical electromagnetic induction (EMI) sensor to create HMZ; ii) the decision on “when” and “how much” irrigation to apply for the different HZ using, soil moisture probes, an agro-hydrological model and weather forecasting; iii) the implementation of a VR irrigation strategy using the pivot speed control, which has been shown to be more practical and cost-effective for farmers. Secondly: to scale up the VR approach to the whole farm and assess on a multi-year period (2016–2021) the benefits in terms of water and energy savings. To achieve this, a semi-distributed agro-hydrological model was implemented that exploited spatial crop phenometrics (i.e., phenological estimates) and the dynamics of growth parameters derived from remote sensing in order to describe real crop evolution. In order to quantify the water and energy savings at the two spatial scales, the estimates obtained using the precise irrigation approach were compared with the farm’s usual irrigation management practices.

2. Materials and methods

2.1. Study farm

The research activity was carried out on the “La Canova” farm in Gambara (Brescia), which is a large livestock farm located in the centre of northern Italy’s cereal-growing area (Fig. 1a). “La Canova” uses 300 ha of land to grow forage cereals for its cattle. In each irrigation

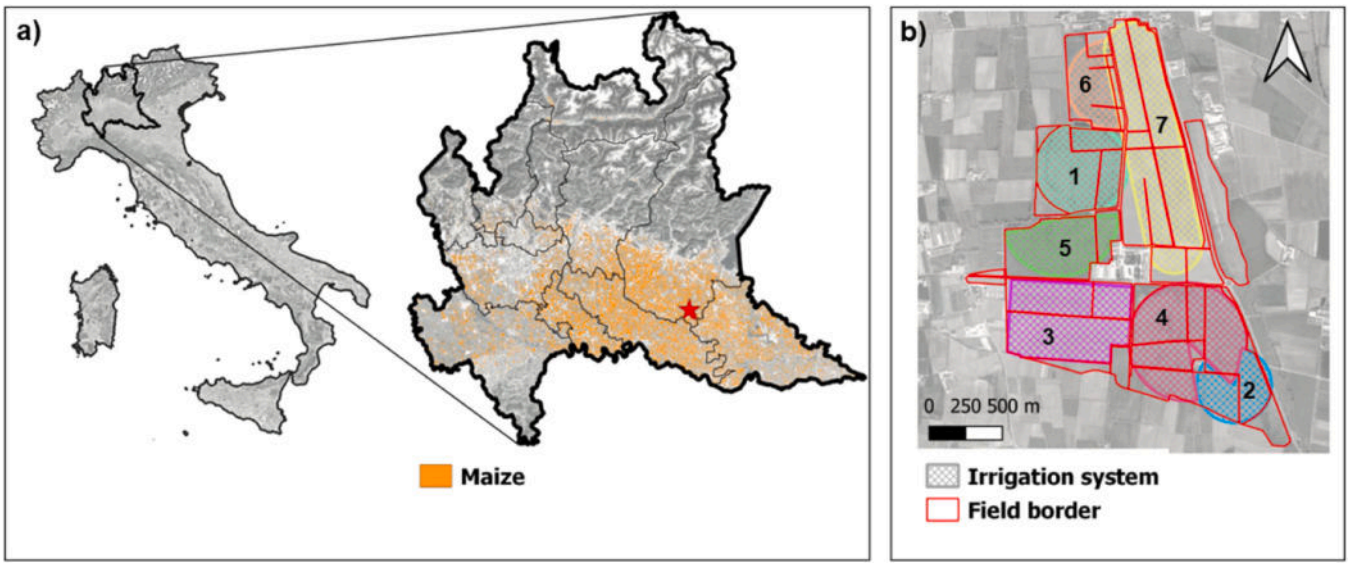

Fig. 1. Study area context: a) location of "La Canova" farm (red star); orange colour highlights the maize-growing area in 2020, according to Lombardy Region soil-use data; b) "La Canova" farm fields (red borders) and sprinkler irrigation systems (dashed areas; each colour identifies a different irrigation system, with the following names: 1 = Rossina; 2 = Vallona Sud; 3 = Vigneto; 4 = Vallona Nord; 5 = Giuseppina; 6 = Muraglia; 7 = Universal).

season, half of the farm area is devoted to maize and the other half to soya bean, according to the following crop rotation: 1st year: maize (grain or silage maize); 2nd year: barley + s harvest soya beans; 3rd year: maize (grain or silage maize); 4th year: soya beans or other fodder crops + second harvest soya beans.

As for irrigation, the farm, which is characterised by nearly flat topography, is mostly served by seven sprinkler systems (center-pivot and lateral move-sprinklers, Fig. 1b). Small residual areas that are not reached by the sprinklers are irrigated by border irrigation or hose reel irrigation.

In the farm, maize is typically irrigated providing a depth of 25–30 mm (depending on the crop development stage) every 4 days, implementing a fixed rotational schedule.

According to the Köppen-Geiger classification system (Kottek et al., 2006), the study site has a humid subtropical climate (Cfa). Due to its geographical location and the morphology of the Po Valley, the site experiences hot, humid summers with sudden thunderstorms and cold winters with diurnal fog and abrupt frost. Agro-meteorological data series were collected from ARPA Lombardia (Regional Environmental Protection Agency of the Lombardy region) station located in Gambara (Lat 45°14', Lon 10°17', about 3 km from the study site) for the period 1993–2021 (Fig. 2). Maximum daily temperatures in July and August are usually above 30°C, while average minimum and maximum values of air humidity are 41 % and 85 % respectively. Average wind speed in the same months is around 1 m s^{-1}. The agricultural months (April–September) are characterised by low rainfall, with an average monthly amount of around 50 mm, dropping to less than 30 mm in July. Reference evapotranspiration (ETo) was calculated using the FAO-56 Penman–Monteith equation (Allen et al., 1998), which estimates ETo for a hypothetical reference grass crop under well-watered conditions. The average monthly ETo in the three central months of the season is approximately 150 mm (Fig. 2).

Fig. 3 shows the monthly cumulative rainfall and ETo values for the six years considered in this study (2016–2021). The rainfall values were recorded by a rain gauge located on the farm. The data show the large variability in rainfall distribution that can occur during the growing

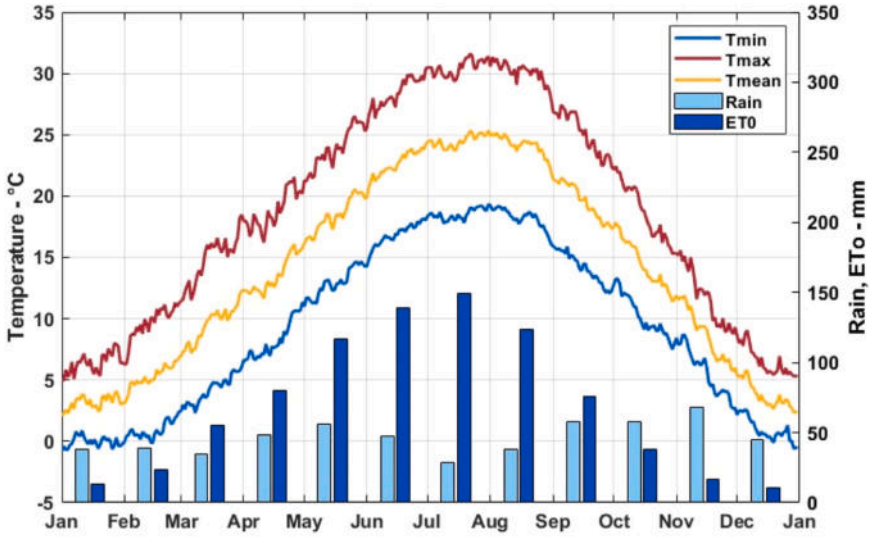

Fig. 2. Daily mean maximum and minimum air temperatures and monthly mean rainfall and ETo at the Gambara meteo station in the period 1993–2021.

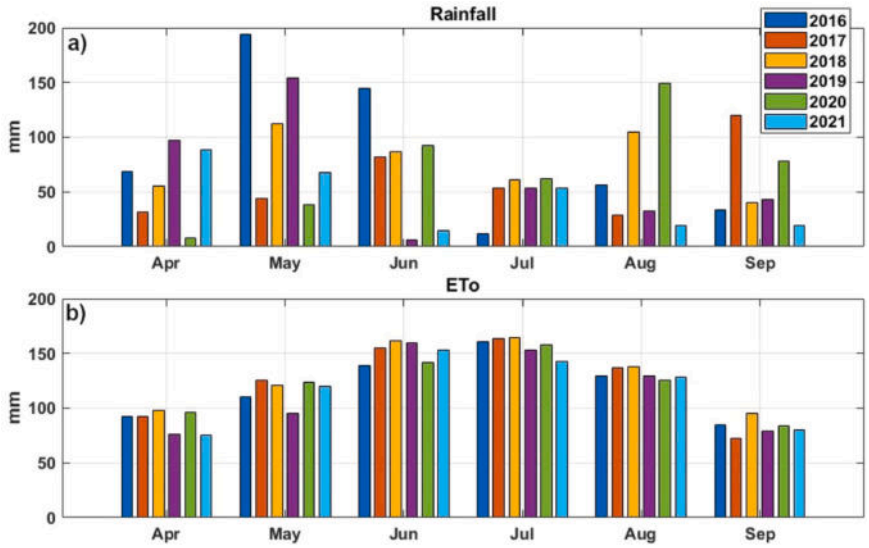

Fig. 3. Monthly cumulative values of a) rainfall and b) reference evapotranspiration (ETo) for the six years considered in this study (2016–2021).

season, while the ETo pattern is fairly constant over the years.

2.2. Soil characterization

A soil survey was carried out over the whole "La Canova" extension. Soil variability was first investigated using an electromagnetic induction (EMI) sensor towed by a quad bike (CMD-MiniExplorer, GFS Instruments; EMI survey executed by AgriSOING s.r.l.). The CMD-MiniExplorer acquires soil electrical resistivity (ER) values for three different soil depths: 0–50 cm, 0–100 cm and 0–180 cm. ER is closely related to the soil physical and hydrological properties (Gupta et al., 2019), so that it can be used to map the soil spatial heterogeneity (Banton et al., 1997; Corwin and Lesch, 2003; Corwin and Plant, 2005). ER values were collected at points along parallel lines and ER maps (one for each investigated soil depth studied) were obtained by interpolating ER points over the farm extension. Finally, the ER maps were processed by cluster analysis techniques using the MZA software (Management Zone Analyst, Fridgen et al., 2004) to identify areas characterised by soils with homogeneous properties. The farm area was thus divided into Homogeneous Soil Zones (HSZs), within which a variable number of suitable sampling points was selected so as to capture the range of electrical resistivity variability observed in each HSZ. For each sampling point, soil samples were taken using a traditional hand auger and the soil stratigraphy was reconstructed to a depth of 1 m. Disturbed samples were collected at depths corresponding to the centre of each soil horizon (typically two to four were identified in the first metre of soil). Laboratory analyses were then performed to determine the gravel content by sieving (particles > 2 mm) and the soil texture by the Bouyoucos hydrometer procedure (the fine earth fraction < 2 mm is subdivided into sand, 0.05–2 mm, silt, 0.002–0.05 mm, and clay, < 0.002 mm), while organic carbon content was measured only in the topsoil by oxidation method (official methods indicated in IMA, 1999).

Based on the textural properties of the sampling points belonging to each HSZ, the HSZ was classified within the following two main classes: "coarse soil unit" or "medium-fine soil unit". Finally, a soil map with two main classes ("medium-fine" soils and "coarse" soils) was produced for the whole farm area.

2.3. Identification of the irrigation sectors

The soil map produced through the soil survey was then used to split the area under each irrigation system into a variable number of Homogeneous Management Zones (HMZs), designed following the sprinkler system geometry and containing a predominant soil type ("medium-fine" or "coarse"). In this specific case, HMZs represent the irrigation sectors where irrigation can be applied at different rates according to soil characteristics.

As for the pilot pivot, identified as pivot number 2 (Vallona Sud) in Fig. 1b and located in the south-eastern part of the farm, the same approach was applied and the area under the irrigation system was divided in two HMZs characterized by different soil types. In addition, in order to make a comparison with the irrigation management commonly adopted in the farm, the two identified zones were further divided into two, for a total of four HMZs, two managed by the farm agronomist ("control" zones) and two according to the methods explained later in this paper (VR sectors). In each HMZ, FDR (Frequency Domain Reflectometry) soil water content probes (Netsens TerraSense, Italy) were installed in two points at two depths, 20 and 40 cm from the soil surface, to monitor the soil water status of the rooted soil profile. Indeed, according to the experience of the farm's agronomist and the literature (Dehghanisanij and Kouhi, 2020; Gao et al., 2010; Mahgoub et al., 2017), maize root density under sprinkler irrigation typically increases down to about 20–30 cm, reaches its maximum within this layer, and gradually declines with depth, with roots commonly extending to 45–50 cm. The wireless sensor network (WSN) of FDR probes was connected to a transmission unit that sent data to a master station near the field, which in turn sent the collected dataset to a server at hourly intervals for remote viewing via a web portal. In the 2021 season, the pivot was equipped with an updated control panel (ICON 5, Valley), which allowed the system speed to be varied and thus the irrigation depth to be changed over the identified HMZs under the pivot. In particular, in the two VR sectors irrigation was managed with the support of soil moisture probes and an agro-hydrological model fed with weather forecasts, while in the corresponding two "control" zones, irrigation was managed according to the usual practices adopted in the farm (25–30 mm of irrigation every 4 days, depending on the crop stage).

For the remaining farm irrigation systems, irrigation events and depths were simulated using the agro-hydrological model calibrated and validated in the pilot pivot, applied in a semi-distributed mode.

Model parametrization for both the pilot pivot and the other farm irrigation systems is described in the following sections.

2.4. Irrigation management in the pilot pivot – real time simulations

The irrigation management of the pilot pivot was guided by an agro-hydrological model implemented with locally acquired data.

Simulations were performed with the SWAP model (Soil-Water-Plant-Atmosphere, Kroes et al., 2017), a mechanistic agro-hydrological model widely used to simulate vertical water fluxes and balances in vegetated areas.

SWAP describes one-dimensional water movements in the soil profile by numerically solving the Richards equation (Eq. 1), modified to account for the root water uptake:

$$\frac{\partial \theta}{\partial t} = \frac{\partial}{\partial z}\left[K(\theta)\left(\frac{\partial h}{\partial z} + 1\right)\right] - S(h) \quad (1)$$

where: θ represents the volumetric soil water content [$L^3\ L^{-3}$]; t is the time [T]; z represents the vertical coordinate (L), positive downward; K (θ) denotes the unsaturated hydraulic conductivity [$L\ T^{-1}$], function of θ; h represents the soil water pressure head [L] and $S(h)$ is the sink term representing crop water uptake by roots [T^{-1}].

In SWAP the sink term is distributed over the root zone according to root density and it decreases under soil water stress. This limits root water uptake when the soil is either too dry or nearly saturated, in accordance with the stress model proposed by Feddes et al. (1978). Potential root water uptake equals potential transpiration. The latter term is derived from the potential evapotranspiration estimated by the model through partitioning evaporation and transpiration according to the temporal evolution of the leaf area index (LAI). Actual transpiration, which corresponds to actual root water uptake, and actual soil evaporation are calculated by the model as a function of soil water availability. Root distribution and length, LAI, crop coefficient (Kc) and crop stress function parameters are crop-specific and vary with growth stage, enabling the model to realistically simulate soil–plant water interactions.

Since the 1970s the model has been extensively applied to simulate water and nutrients transport in the soil (Li and Ren, 2019; Singh et al., 2006), and to estimate crop water needs to support irrigation optimization for several crops, including maize (Bonfante et al., 2019, 2015; Jiang et al., 2016; Monaco et al., 2014; Pan et al., 2020; Yuan et al., 2019). SWAP requires agro-meteorological inputs, a vertical schematisation of the soil profile completed with the hydraulic properties of the different soil horizons, crop development parameters and information about the groundwater depth, and allows the simulation of soil water status dynamics, evaporation, transpiration, capillary rise and deep percolation under different irrigation strategies. Irrigation can be prescribed as observed irrigation events or predicted through the irrigation scheduling option, which automatically triggers irrigation when user-defined conditions are met, such as the attainment of threshold values of soil water content or soil water potential.

To obtain the necessary data, an agro-meteorological station (Netsens MeteoSense, Italy) was installed in the farm close to the pilot pivot. To investigate the potential presence of a shallow groundwater table in the area, the regional groundwater depth data provided by ARPA was examined. In addition, to identify the potential impacts of local irrigation practices on the groundwater table, two 2.5 m-long piezometers equipped with pressure transducers were installed on the farm.

The database obtained through the analysis of soil samples collected in the field was integrated with the information available in the Lombardy regional soil database linked to the soil map 1:50.000 (LOSAN Soil Database, ERSAF, n.d.). As explained in Section 2.2, some properties (such as the organic carbon content) were detected in the collected soil samples only for the topsoil horizons; for this reason, every HSZ was referred to the most similar cartographic unit in the regional soil map to complete the missing information for the deeper soil horizons. The van Genuchten-Mualem soil hydraulic parameters required by SWAP for the soil horizons of each soil profile were then estimated starting from the physical-chemical characteristics of the different horizons by applying the Rosetta3 Pedo-Transfer Function (PTF) set (Zhang and Schaap, 2017). Rosetta is a hierarchical set of pedo-transfer functions which applies different models depending on the available input data (soil texture, bulk density, volumetric water content at field capacity, volumetric water content at wilting point). The chosen Rosetta model was the one requiring the soil texture and bulk density as inputs; bulk density was estimated by applying the PTF proposed by Pellegrini (Pellegrini et al., 2007) which requires clay, sand, and organic carbon contents as inputs.

The SWAP model was implemented for each point in which the soil moisture probes were installed in the pilot pivot (i.e., eight points). The crop parameter patterns were derived from other studies conducted under similar geographical conditions, in particular, the LAI and Kc values were obtained from Facchi et al. (2013) and were as follows: $LAI_{max} = 5.7$, $Kc_{ini} = 0.28$, $Kc_{mid} = 1.14$, $Kc_{end} = 0.57$. The thermal sums required by SWAP for the Growing Degree Days (GDD) model used to estimate the crop development stages (DVSs) were set according to Pampana et al. (2009). The maize crop in the two fields under the pilot pivot was a Pioneer variety (P0937) FAO 500 maturity class, sowed on 2 and 3 April 2021. Emergence occurred on 20 April, flowering around 3 July, and the two fields were harvested on 9 and 10 September, respectively.

The model results were processed to extract the soil water content series at the depths at which the moisture probes were installed (i.e., 20 cm and 40 cm). The simulated values were then compared to the measured soil water content. During the first part of the season (10 June–1 July) the measured series were used to manually calibrate the following hydrological properties: soil water content at saturation (θ_{sat}) and, for coarse soils, saturated soil hydraulic conductivity (K_s) of the upper soil horizon. These parameters were then kept constant until the end of the season. From 1 July to 22 August, probe data were used to validate the model. For the calibration and validation phases, three performance indices were selected and calculated: Root Mean Square Error (RMSE), Nash-Sutcliffe Model Efficiency (NSME) and Median Absolute Error (MedAE).

The "reference" irrigation scheduling for the pilot pivot and the other irrigation systems on the farm is based on fixed rotational turns, since the water pumped from the 12 wells is insufficient to activate all seven irrigation systems simultaneously, and, moreover, the movement of the different irrigation machines is not independent (e.g., some machines may only start once others reach a certain position). The farm tenant imposed the following constraints on the study, in particular: 1) maintaining the scheduled fixed irrigation turns throughout the season, 2) not skipping them (except for the last irrigation intervention before harvesting), 3) providing a minimum irrigation depth of 25–22 mm for the coarse and fine sectors at the beginning of the season, and 22–18 mm from July onwards at each irrigation turn; 4) providing three fertigation interventions of 30 mm uniformly across all irrigation sectors on 12, 21 and 25 June.

Seven-day weather forecasts, provided by ABACO S.p.A and calibrated to the weather station installed in the farm, were downloaded on a daily basis using a Python script developed for this purpose. In the pilot pivot the SWAP model was run after each irrigation turn using the weather forecasts to simulate the soil water content dynamics until the next irrigation turn. This allowed the optimal irrigation depth to be identified in advance. The optimal irrigation depth is defined as the amount of water required to refill the rooted soil zone to field capacity, to be provided to the different HMZs. In the SWAP model, field capacity (FC) was calculated by assigning a soil water pressure head in the crop input file. This was then used to calculate the corresponding soil water content through the van Genuchten–Mualem soil hydraulic functions. For the simulations, the FC potential was set according to the observed soil type at each sampling point, following Vianello and Ciavatta (1989): −330 cm for clay soils, −200 cm for loamy soils and −170 cm for sandy-loam soils.

Knowing the irrigation depths to be delivered to each sector in advance was requested by the farm agronomist, because the movement of the different irrigation machines is not independent and therefore a farm plan must be prepared in time.

Simulation outputs were processed to calculate the water deficit between field capacity and the actual water content in the rooted zone (whose thickness was dynamically calculated according to the root deepening in time). This deficit, divided by the irrigation method efficiency estimated as 80 % for sprinkler irrigation by means of pivot, gave the water amount to be provided in the following irrigation turn in each specific soil unit (HSZ). Since two homogeneous soil zones (HSZs) were monitored through the installation of soil water content sensors in each HMZ, two SWAP simulations were run for each HMZ (one for each HSZ). The irrigation depth to be applied to each sector in the subsequent irrigation event was calculated as the weighted average of the two values obtained from the simulations of each HSZ within the sector, weighted by their respective surface areas.

A MATLAB© script was developed to gather all the necessary data (weather forecasts, soil and crop data), format it in the required SWAP input files and run simulations for the different irrigation sectors and soil types. The same framework also enabled output data to be analysed and displayed in the form of plots and summary tables.

2.5. Yield monitoring in the pilot pivot

At the end of the 2021 agricultural season the crop in the two fields below the pilot pivot was harvested with a CLAAS LEXION 750 (CLAAS KGaA mbH, Harsewinkel, Germany) harvester equipped with a GPS system and sensors to measure and map grain weight and humidity. At the beginning of the harvesting operations, harvested grains were weighted to calibrate the harvester sensor.

The yield map was provided as a layer of points in which the yield measured by the sensor and its humidity were associated to each point. In order to make the yield values comparable over the whole harvested surface, they were corrected to account for the grain humidity. Thus, yields were recalculated considering a standard grain humidity value of 14 %.

Data points were analysed and outliers removed, thus the points were interpolated (using the inverse distance weighted method) on a 5 m grid to obtain a continuous map over the fields. At the end of such elaborations, average yield values for each irrigation sector were calculated, excluding values on the field borders to avoid edge effects.

2.6. Irrigation management scenarios at the farm scale

The model implemented for the pilot pivot was then applied to the whole farm to simulate two optimized irrigation scenarios for a 6-years period (2016–2021).

A modelling framework was developed in MATLAB© to apply SWAP following a semi-distributed approach to the seven sprinkler systems in the farm. A GIS (Geographic Information System) database was implemented with all the available data provided by the farm agronomist, including: field and irrigation system boundaries; land use and crop rotations; irrigation dates and amounts; crop varieties; sowing and harvesting dates; seeding density; fertilizer management; yield. Moreover, the agro-climatic daily data series registered by the ARPA Lombardia at the Gambara station were collected, their quality assessed and gap-filled using data sets recorded at neighbouring stations. Finally, Sentinel-2 (S2) satellite imagery (Level 2 product; BOA – Bottom-Of-Atmosphere – reflectances) of the study area were downloaded from Copernicus Open Hub and Level 3 (L3) products generated (see Section 2.6.1). SWAP was applied for each year of the period 2016–2021 to the HMZs identified as described in Section 2.3. To avoid disrupting the company's organisation and to ensure that the proposed approach is straightforward to use - given the current interdependency of the irrigation machines - simulations were run for each irrigation sector maintaining the same dates as in the farm management schedule, while irrigation depths were optimized as explained for the pilot pivot. The MATLAB© framework allowed to run a sequence of simulations in a cycle, each simulation ending in a date when the actual irrigation took place. In every step two simulations were launched for every HMZ, one for each soil type. At the end of the two simulations, the water deficit with respect to the field capacity was calculated and, to be even more conservative than for the pilot pivot, the higher of the two irrigation depths divided by the efficiency of the irrigation method was applied at that irrigation turn.

2.6.1. Remote sensing data and analysis

Occurrence of phenological estimates (phenometrics) and LAI time series, L3 products, were obtained by processing S2 images acquired for the period 2016–2021. The Sen2r toolbox (Ranghetti et al., 2020) was used to download and pre-process images by sub-setting the area corresponding to the farm estate and masking clouds using Scene Classification maps (SCL) and quality indicators for CLouD probabilities (CLD; TAS Team, 2021) information provided with S2 imagery. Maps of MSAVI2 (Modified Soil-Adjusted Vegetation Index, Eq. 2) were calculated and analysed with the Sen2rts package (Ranghetti, 2022).

$$MSAVI2 = \frac{2 * b8 + 1 \quad - \sqrt{(2 * b8 + 1)^2 - 8 * (b8 - b4)}}{2} \tag{2}$$

where b4 and b8 are the reflectance values in S2 bands 4 (red, 665 nm) and 8 (near-infrared, 833 nm), respectively.

Sen2rts is a R package developed by CNR-IREA that allows the i) the extraction of vegetation indices or biophysical parameters (e.g., LAI) for a specific area of interest, ii) the smoothing and gap-filling to generate a time series, and iii) the interpolation of a double logistic for curve analysis. From the reconstructed MSAVI2 time series first crop cycles, summer vs. winter crops, are identified and then the occurrence of phenological stages is automatically estimated based on a curve analysis approach; for details see Ranghetti et al. (2021). The phenometrics derived from *Sen2rts* toolbox were: start of the season (SOS), 10 % of soil cover (fc_10), flowering (flower), position of peak (pop), position of the maximum value (maxval), senescence (sen) and end of the season (eos). Remotely sensed phenometrics were then used to identify the crop growth stages required by SWAP model (dates of crop emergence, flowering and maturity) for each simulation unit. Subsequently, LAI maps were obtained using the SNAP toolbox (Sentinel Application Platform, European Space Agency), and spatial average for each simulation unit were extracted to obtain time series to be used as input in SWAP.

Finally, specific information on maize hybrid (type of hybrid, FAO maturity class, sowing and harvesting dates for every simulation year) provided by the farmer, together with S2 derived phenometrics, were used to verify the thermal sums proposed by Pampana et al., 2009 for the Growing Degree Days (GDDs) model used to simulate crop development in SWAP.

3. Results and discussion

3.1. Soil characterization

Interpolated electrical resistivity maps for the three depths investigated by the EMI sensor are shown in Fig. 4, where colours from red to green represent increasing values of electrical resistivity. Cluster analysis performed on the three ER maps resulted in a map consisting of 10 Homogeneous Soil Zones (Fig. 5) characterised by soils with similar hydrological properties. The HSZ codes reported in Fig. 5(e.g., DAM1, DAM2) were assigned by associating each zone with the most similar cartographic unit of the 1:50.000 regional soil map of Lombardy (LOSAN database).

The locations where the soil samples were collected are marked with a black dots in Fig. 5. A total of 44 points were selected for the traditional soil sampling to cover the spatial variability of electrical conductivity (EC) in each HSZ. The main physical properties of the "representative" soil profile for each HSZ are given in Table 1. Where

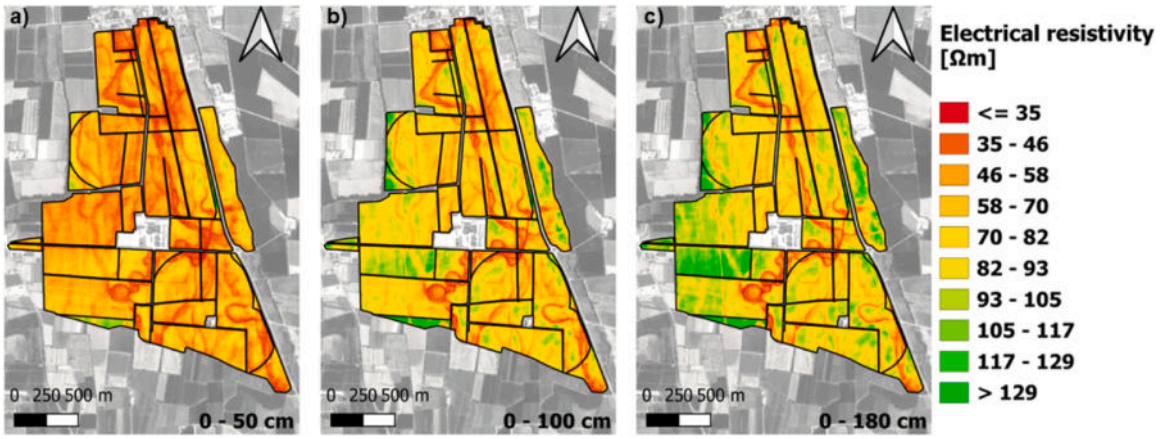

Fig. 4. Interpolated electrical resistivity maps for the three survey depths recorded by the Electro-magnetic Induction (EMI) sensor: a) 0–50 cm layer; b) 0–100 cm layer; c) 0–180 cm layer.

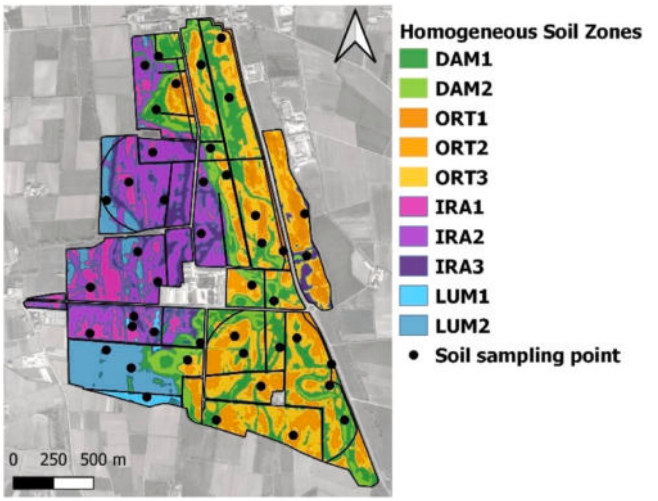

Fig. 5. Homogeneous Soil Zones (HSZs) identified using cluster analysis on electrical resistivity maps. The black dots represent soil sampling locations.

more than one profile was present in an HSZ, the soil properties were obtained by averaging the values measured at each depth for the profiles belonging to that HSZ. The the last column shows the soil type (fine or coarse) assigned to each HSZ according to the soil texture.

As shown in the previous map and table, the “La Canova” farm is characterised primarly by coarse soils. The predominant soil texture is sandy loam in the shallower layers becoming coarser with depth. Many of the farm’s soil contain a high percentage of gravel, with the exception of the HSZs DAM1, DAM2, IRA2 and IRA3. These HSZs are located mainly along the course of paleochannels that cross the farm from north to south. They are characterized by the presence of layers with loam and clay-loam textures in the first two horizons, at least. These four HSZs were therefore classified as “fine” soil units, while the other six as “coarse” soil units.

Fig. 6a shows the map illustrating the spatial distribution of the two soil macro-types. Based on the distribution of ”fine” and ”coarse” soil types, and following the geometry of the seven sprinkler irrigation systems, the area under each system was divided into sub-areas characterized by a predominant soil type. Twenty-nine irrigation sectors (HMZs) were identified, shown with blue lines in Fig. 6b. Each “coarse” or “fine” sub-area within an HMZ was then associated with the predominant soil unit (HSZ) within that management zone. This means that, within in each HMZ, all ”coarse” soil units were associated with the ”coarse” HSZ covering the larger area, and the same applied for the ”fine” soil units.

As for the pilot pivot, four HSZs were observed (Fig. 7a): DAM1, DAM2 (light and dark green in the figure), ORT2 and ORT3 (yellow and orange in the figure), the first two belonging to the “fine” macro-type, while the other two to the “coarse” macro-type. The subdivision of the pivot area was done as shown in Fig. 7b: two areas with a dominant soil type were identified, but each one was further subdivided in two (for a total of four sectors) to obtain a VR sector and a control sector for each soil type. The northern part of the pivot area was not considered as it is watered by a different irrigation system.

Locations where the Netsens soil moisture sensors were installed are reported in Fig. 7c (blue stars).

3.2. *Irrigation management in the pilot pivot – real time simulations*

3.2.1. *SWAP model implementation, calibration and validation*

For the 2021 season, the SWAP model was implemented for the four locations where soil moisture sensors had been installed: precisely in the sectors managed by the application of the model (i.e., locations number 1, 2, 7 and 8 in Fig. 7c). The SWAP model was implemented using the meteorological and soil data described in Section 2.4. At the soil surface, the upper boundary condition was set as a flux boundary, driven by rainfall and irrigation inputs. At the lower boundary, free drainage condition was applied, since regional groundwater was located well below the simulated soil profile (8/10 m deep) and did not affect the soil water balance during the study period. This was also confirmed by the piezometers installed on the farm, which remained consistently dry throughout the season.

The soil water contents simulated by SWAP at 20 and 40 cm depth were extracted from the results of the simulation and compared with the soil water contents measured by the Netsens sensors at the same depths. During the calibration period, the saturated water content (θ_{sat}) of the upper soil horizon at all four sites was adjusted within a range of ± 10 %, to align with the water content values measured by the sensors. For the two sites with coarse-textured soils (points 1 and 2), the saturated soil hydraulic conductivity (K_s) of the upper soil horizon was increased by 20 % to improve the fit between the simulated and observed data.

Fig. 8 shows the performance of the model over the whole irrigation season for the four sites. Table 2 shows the Median Absolute Error (MedAE), the Root Mean Squared Error (RMSE) and the Nash-Sutcliffe Model Efficiency (NSME) indices, which were calculated using the hourly output and measured data of soil water content from the calibration and validation periods.

As shown in Fig. 8, the moisture probes required a period of adjustment following their installation. Between installation at the end of April and the first irrigation on 13 June, there was insufficient rainfall

Table 1
Physical properties of the Homogeneous Management Zones (HSZs) identified for the whole farm area and their classification in coarse or fine units (TXT = textural class. L = Loam; CL = Clay Loam; SL = Sandy Loam; S = Sand; LS = Loamy Sand).

HSZ code	Layer	Sand (%)	Silt (%)	Clay (%)	Gravel (%)	TXT	Organic carbon (%)	Class
DAM1	0–35	38.5	35.5	26.0	15.8	L	1.69	Fine
DAM1	35–55	42.1	29.9	28.0	15.7	CL	0.70	
DAM1	50–110	63.4	22.3	14.3	31.5	SL	0.10	
DAM2	0–30	40.3	36.9	22.9	7.8	L	1.86	Fine
DAM2	30–60	30.2	38.8	31.0	7.0	CL	0.70	
DAM2	60–90	22.7	45.7	31.7	3.8	CL	0.10	
DAM2	90–110	35.7	42.0	22.3	23.3	L	0.10	
IRA1	0–30	58.4	26.1	15.4	7.0	SL	1.38	Coarse
IRA1	30–60	57.8	24.2	18.0	9.2	SL	0.70	
IRA1	60–110	90.0	7.8	2.2	19.0	S	0.10	
IRA2	0–30	44.4	34.1	21.5	4.7	L	1.52	Fine
IRA2	30–50	44.7	29.3	26.0	4.3	L	0.70	
IRA2	50–110	87.3	9.7	3.0	11.0	S	0.10	
IRA3	0–30	37.0	37.2	25.9	5.4	L	1.56	Fine
IRA3	30–60	33.2	35.4	31.4	5.4	CL	0.70	
IRA3	60–80	61.4	22.4	16.2	13.0	SL	0.10	
IRA3	80–110	80.3	15.5	4.3	17.5	LS	0.10	
LUM1	0–45	74.8	16.4	8.8	2.5	SL	1.56	Coarse
LUM1	45–100	89.0	9.5	1.5	1.5	S	0.70	
LUM2	0–45	58.0	24.0	18.0	15.7	SL	1.57	Coarse
LUM2	45–100	81.0	11.3	7.7	21.7	LS	0.70	
ORT1	0–30	68.8	18.6	12.6	30.0	SL	2.12	Coarse
ORT1	30–50	73.0	17.0	10.0	35.0	SL	0.70	
ORT1	50–110	89.3	8.0	2.7	43.3	S	0.10	
ORT2	0–35	53.0	31.2	15.9	21.0	SL	1.77	Coarse
ORT2	35–55	57.8	22.6	19.6	27.0	SL	0.70	
ORT2	55–110	84.8	12.2	3.0	31.0	LS	0.10	
ORT3	0 – 40	47.2	30.2	22.7	38.0	L	2.03	Coarse
ORT3	40 – 60	66.5	17.5	16.0	60.0	SL	0.7	

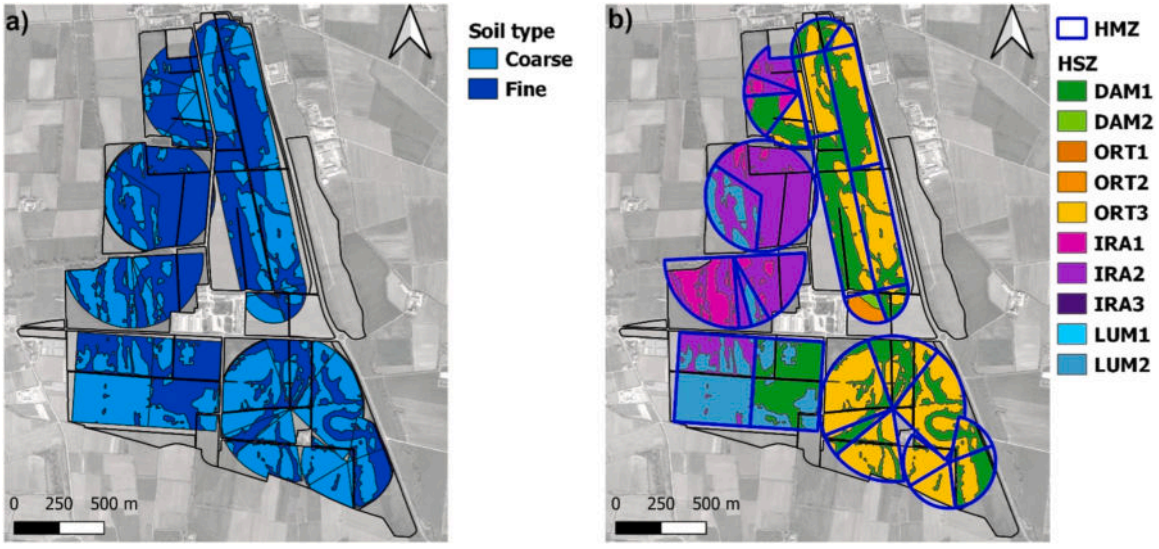

Fig. 6. Spatial distribution of soil types on the "La Canova" farm: a) soil macro-types ("fine" and "coarse" soils), field boundaries are shown in black; b) irrigation sectors (HMZs) are shown in blue, each "fine" and "coarse" HSZ in the sector is associated with the dominant "fine" or "coarse" soil unit (HSZ) according to the map in Fig. 5.

to strengthen the hydraulic contact between the soil, disturbed by the installation, and the probe tips. Data collected during this period were therefore excluded from the analysis.

In the first phase of the simulation (calibration period), there was an underestimation of the soil moisture at 40 cm (light orange lines) at points 1 and 2. This was probably due to the initial conditions of the model being set incorrectly, resulting in the lower layers being more humid than expected despite the low rainfall during the 2021 season. The fit between the simulated and observed data improved significantly after the first four irrigations. Points 2 and 7 demonstrated the best performance, with highly satisfactory values for all indices (low MedAE and RMSE values, and rather high NSME), particularly at a depth of 20 cm. At 40 cm the model's performance at point 2 during the calibration phase was limited by the aforementioned initial condition issue, affecting the early simulation results; this limitation was reduced during the validation phase, resulting in improved model performance. The simulation at point 8 at 20 cm is affected by the peculiarities of the soil in which the probe was installed. In fact, the soil was both plastic and very compact, making installation difficult; it is therefore likely that gaps were left around the probe tips. This is probably the cause of the

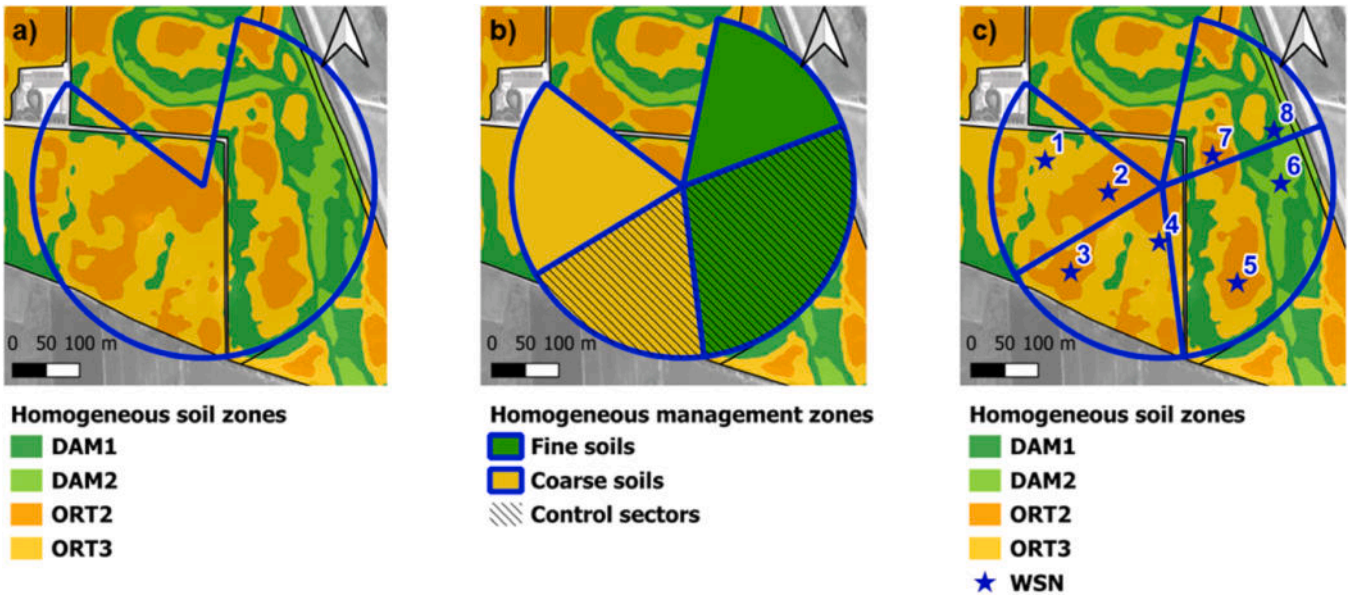

Fig. 7. Pilot pivot: a) area covered by the sprinkler irrigation system; b) sectors (i.e., Homogeneous Management Zones) identified for the pilot pivot: the two main soil macro-types observed were assigned to two different sectors (green for "fine" soils and yellow for "coarse" soils) which were further subdivided to obtain two VR sectors (solid fill) and two control sectors (dashed fill); c) locations of Netsens sensors (wireless sensor network - WSN) in the pilot pivot.

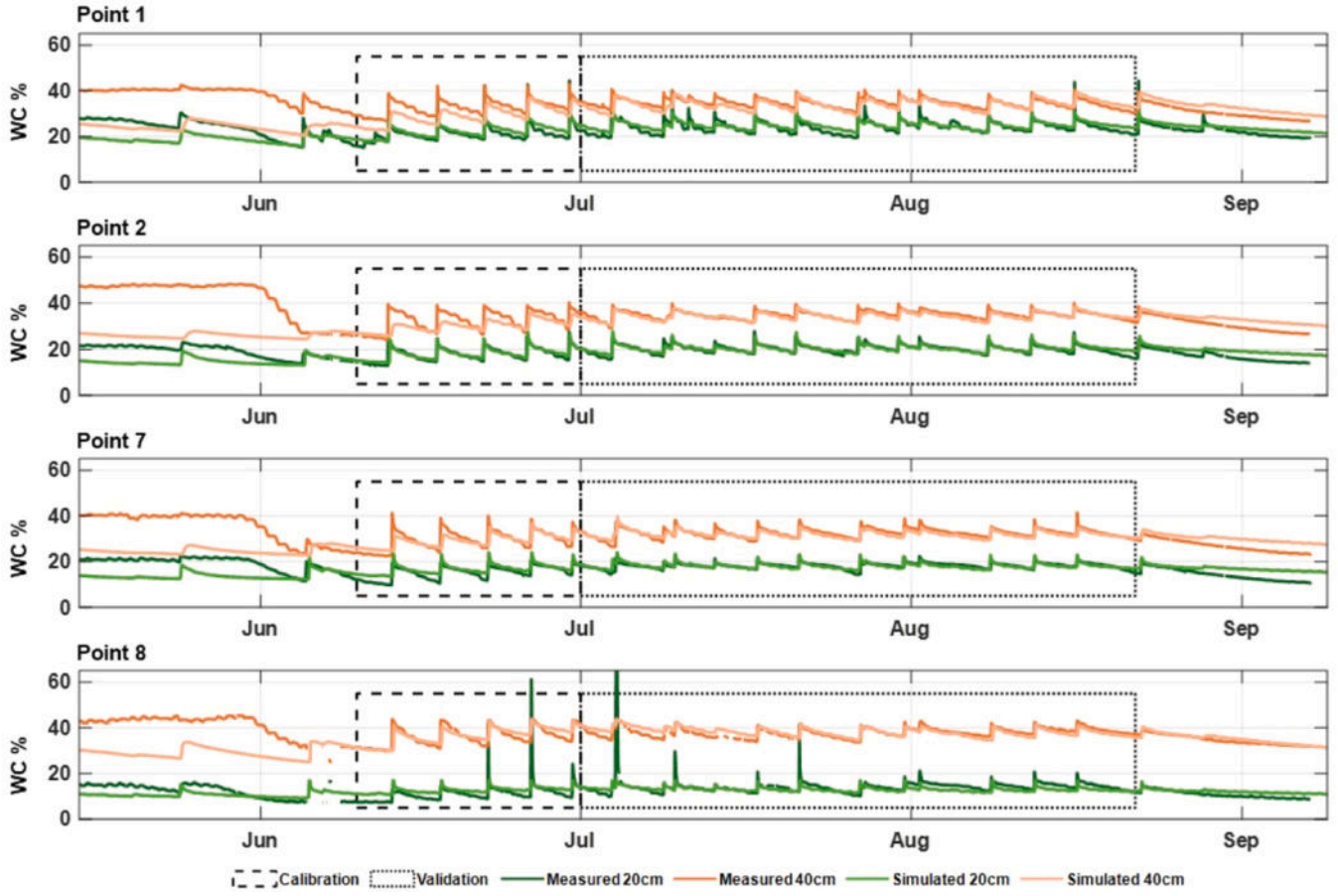

Fig. 8. Soil water content model outputs (light coloured lines) and values measured by the Netsens sensors (dark lines) at depths of 20 and 40 cm at the four sites managed through the SWAP model (see Fig. 7c for their location). The dashed box indicates the calibration period (10 June–1 July), and the dotted box the validation period (1 July–22 August).

spikes in the humidity readings seen in the series recorded by the probes (a sudden increase in water content up to 65 %, followed by an equally rapid decrease). Such behaviour is unreasonable for the soil and can not be simulated by the model; it led to low NSME and high RMSE values

Table 2
Model performance indices calculated for the calibration and validation periods: Median Absolute Error (MedAE), Root Mean Square Error (RMSE) and Nash-Sutcliffe Model Efficiency (NSME) index values for the four simulated sites at the two soil moisture probe depths.

		20 cm depth			40 cm depth		
	Simulated point	MedAE (%)	RMSE (%)	NSME (-)	MedAE (%)	RMSE (%)	NSME (-)
Calibration	1	1.09	2.25	0.47	3.52	4.24	-0.80
	2	0.60	1.42	0.74	2.29	3.78	0.20
	7	1.32	2.04	0.45	1.19	2.65	0.57
	8	2.00	3.52	0.18	1.27	2.35	0.65
Validation	1	1.09	1.86	0.52	1.12	1.93	0.02
	2	0.50	1.12	0.62	0.68	1.26	0.45
	7	0.54	0.95	0.42	0.90	1.39	0.51
	8	1.24	3.32	0.07	1.14	1.69	0.28

(both indices are sensitive to extreme values), indicating that the simulation deviates from the measured data at the extreme values of the series.

Although calibration could probably have been improved by adjusting more soil hydraulic and/or crop parameters, it was decided to modify only those strictly necessary to achieve an acceptable result, since the modeling approach was then applied to the entire farm.

Considering the MedAE index, which is less sensitive to extreme values, the performance of the model's performance is generally good. Error values in the validation period are between 0.50 % and 1.24 % for the 20 cm simulations, and between 0.68 % and 1.14 % for the 40 cm simulations.

3.2.2. *Irrigation management*

The fixed irrigation turns established on the farm for the pilot pivot (every four days) were maintained at the request of the farm tenant, so as not to complicate the management of the farm's sprinkler irrigation systems with time-varying turns. At the end of each irrigation cycle, the model was run in the two VR sectors using 7-day weather forecast data as input. The model results in the two soil units for each sector were then processed to calculate the irrigation water required to replenish soil moisture to field capacity during the next irrigation cycle. For each sector, the irrigation depth to be applied in the next round was calculated as the average of the results for the two soil units, weighted by their area. An example of the model output for a single HSZ (in this case the one relating to sensor at location 2 in Fig. 7c) used to calculate the optimum irrigation depth to be applied is shown in Fig. 9. The continuous red line shows the water content of the root zone, which is calculated by integrating the simulated water content over the rooted zone, while the green and red dotted lines represent the soil water contents at field capacity and wilting point, respectively. Although these soil water contents are usually linked to storage-based ("bucket") models, in this case they were derived from the simulated soil water pressure heads. They are used as reference values to interpret soil water status and calculate the optimum irrigation depth. Field capacity was calculated using the Van Genuchten–Mualem model and the potentials defined in Section 2.4, while wilting point was calculated using a potential of −15,000 cm. The resulting values were then integrated over the root zone to provide a reference for irrigation scheduling. The yellow dotted line represents the soil water content when the readily available water (RAW) is depleted (FAO threshold).

The grey box indicates the period during which the simulations are fed with weather forecasts to predict the soil water content for the following days.

As the farm tenant imposed some restrictions on irrigation management, the simulated soil water content was sometimes above the field capacity and often above the FAO threshold (yellow dotted line in Fig. 10).

In the 2021 season, the total amount of irrigation applied to the pilot pivot was 391 in the coarse and 360 mm in the fine sector, while

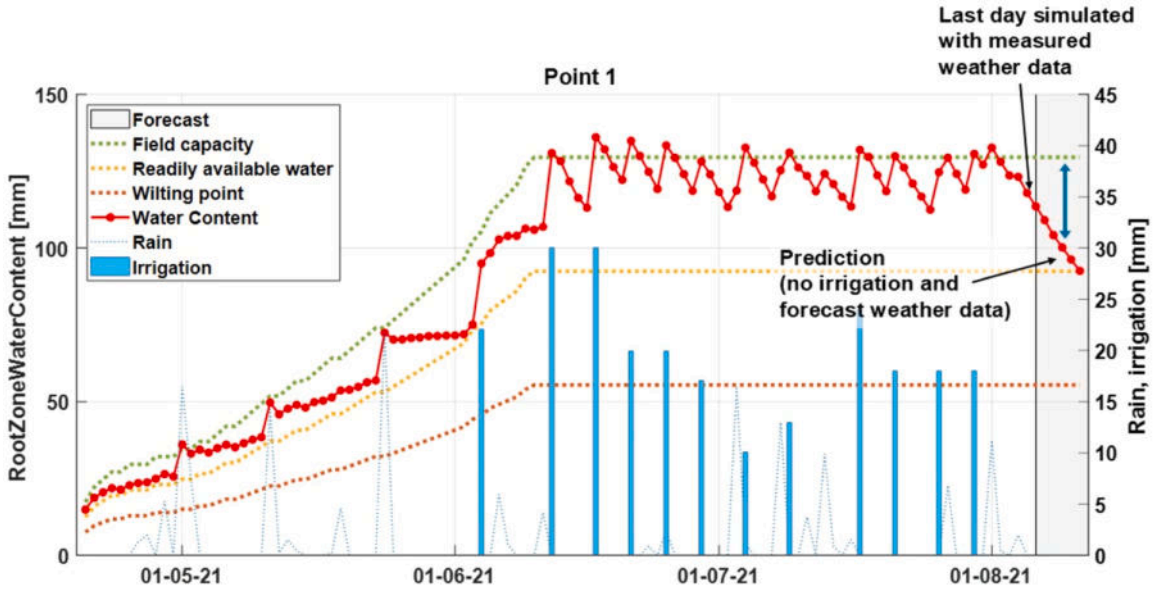

Fig. 9. Example of model output for site 1 (its location is shown in Fig. 7c); the irrigation requirement at the next turn is used together with that simulated for site 2 to calculate the optimum irrigation depth to be applied to the coarse soil sector (difference between field capacity and water content in the root zone, shown with a blue arrow).

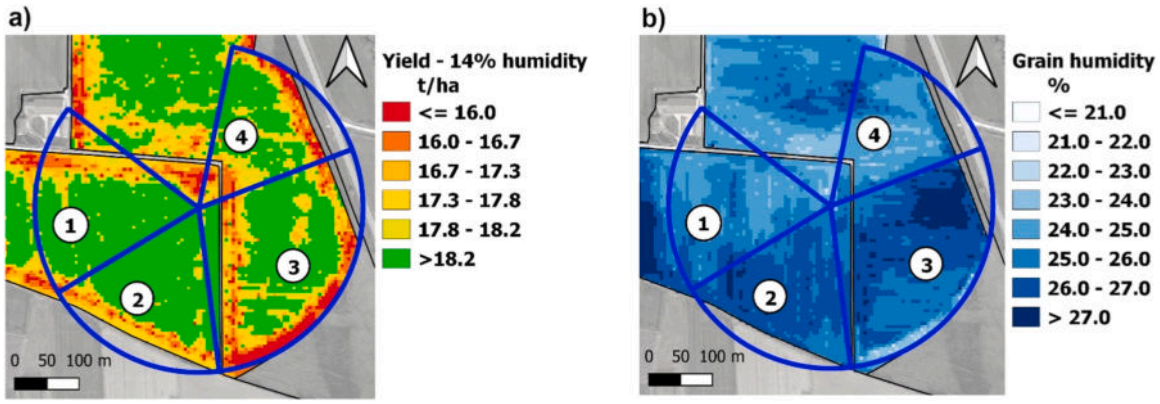

Fig. 10. Maps obtained by processing the point yield maps provided by the variable rate harvester: a) yield map with values corrected to 14 % grain moisture; b) grain moisture map.

469 mm was applied to the control sectors. Using the precision irrigation approach (VR) resulted in a water savings of around 20 % in the pivot (17 % and 23 % in the coarse and fine sectors, respectively). As a reduction in irrigation consumption leads to a corresponding reduction in irrigation time, the estimated average energy saving for groundwater pumping and pivot handling was in line with the water saving percentage.

3.3. Yield map for the pilot pivot

The raster maps of yield and grain moisture produced starting from the point maps provided by the variable rate harvester are shown in Fig. 10a and Fig. 10b, while the mean values of yield achieved in the four sectors are illustrated in Table 3. To avoid boundary effects (i.e., uneven sowing near the boundaries, lower yield in the corridors around the fields), the mean value for each sector was calculated taking into account the intersection of the sector surface with a 20 m buffer around the field boundary.

The results showed no difference in yield (14 % moisture content) between the VR-irrigated sectors (sectors 1 and 4 in Fig. 10) and the sectors irrigated according to the traditional farm schedule and irrigation depth (sectors 2 and 3). Grain moisture was slightly lower in the VR sectors, resulting in further energy savings during grain drying. The grain quality was the same in all four sectors; in particular, no fungal infections were detected in the field (quality data not reported).

3.4. Irrigation management scenarios at the farm scale

3.4.1. RS phenometrics and crop parameters

LAI time series and phenometrics for the two sub-areas in each HMZ for the period 2016–2021 were obtained by analysing S2 data and used to feed the semi-distributed SWAP model.

An example of the i) raw MSAVI2 data, extracted for two simulation units (i.e., 03 and 04) of the VR scenario, and ii) gap filled time series and corresponding phenometrics are shown respectively in Fig. 11a and b. The two upper panels (Fig. 11a), represent with dots the original index value, with their quality assessment (QA) values associated as derived according to cloud probability information. The lower panels (Fig. 11b), report with the black line the gap-filled and smoothed data series and the red line the fitted series (double logistic interpolation). The lower panels also show the phenological stages identified as vertical lines: start of the season (SOS, grey line), 10 % of soil cover (fc_10, red), flowering (flower, cyan), position of peak (pop, orange), position of the maximum value (maxval, blue), senescence (sen, green) and end of the season (eos, dark green). Finally, the identified crop season are indicated by black vertical lines.

Table 3
Average yield data for the four irrigation sectors in the pilot pivot.

Sector	Soil type	Irrigation management	Average yield (t/ha)
1	Coarse	VR	18.43
2	Coarse	Uniform	18.78
3	Fine	Uniform	18.24
4	Fine	VR	18.34

As described in De Peppo et al., 2022, the comparison between the remotely sensed phenological stages and the phenology obtained by a crop model already calibrated and validated for maize in northern Italy (ARMOSA, Perego et al., 2013) led to the following results: the beginning of the season (sos) corresponds to leaf development (BBCH 17) and fc_10 corresponds to the beginning of stem elongation (BBCH 30). Furthermore, the beginning of flowering (flower) falls between BBCH 35 and 40. The peak (pop) of MSAVI2 corresponds to the full flowering stage (BBCH 60). At the end of maize development, the identified senescence (sen) corresponds to the fruit ripening stages (BBCH 80). These observations are considered to be valid regardless of the maize hybrid sown.

Finally, the remotely sensed phenological stages were also compared with those calculated using a simple growing degree day (GDD) model, which used specific thermal sums for each FAO class. Fig. 12a, shows an example of simulation and remote sensing estimates for one of the HMZs used in the 2018 simulations. The dark blue lines represent the smoothed MSAVI2 values for a specific HMZ, while the dotted coloured vertical lines show the simulated crop emergence, flowering and maturity, at the developmental stages (DVS) of 0, 1 and 2, respectively. These were calculated using the GDD model implemented in SWAP, and the grey dashed vertical lines illustrate the stages identified by the sen2rts R package. Reported results show a very good overlap between DVS 0 and sos (start of season), DVS 1 (flowering) and pop (position of peak), and DVS 2 (maturity) and eos (end of season). The same figure shows the crop coefficient (Kc) curve associated with the crop development used in the simulations.

While the Kc values were obtained from the literature, the temporal occurrence and duration of the crop development stages were calculated according to the remotely sensed phenological estimation spatially obtained in each HMZ. Fig. 12b shows the LAI curve for the same HMZ obtained using the SNAP toolbox, which was then used as input for the SWAP simulation. The red dots show the original LAI estimation, while the blue lines illustrate the daily interpolated version provided by sen2rts.

3.4.2. Agro-hydrological modelling results

The modelling framework developed in MATLAB© was applied to all sectors under the seven sprinkler irrigation systems in the period

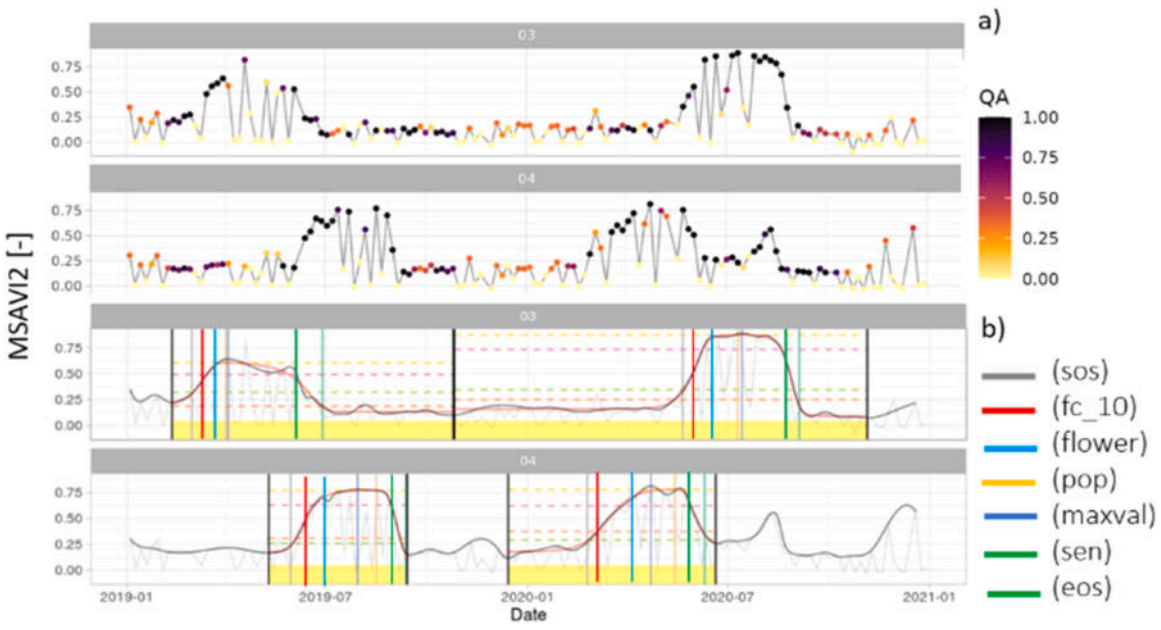

Fig. 11. Sentinel-2 data processing: a) example of vegetation index data for two Homogeneous Management Zones corresponding to two simulation units (i.e., 03 and 04 in figure) with their Quality Assessment (QA) value; b) cleaned, smoothed and interpolated time series used to calculate the crop phenology using the Sen2rts R library; for description of phenological stages see Section 2.6.

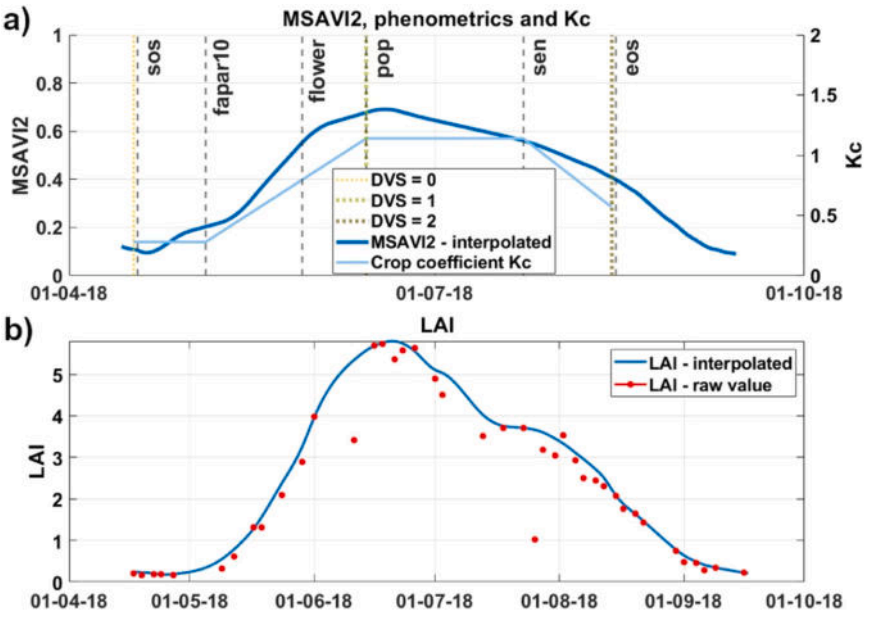

Fig. 12. Example of time series used in the SWAP simulations: a) reconstructed MSAVI2 time series for an HMZ (blue line), phenological estimates obtained with the sen2rts package (dashed black lines) and the growing degree days (GDD) model (coloured dotted lines), and crop coefficient (Kc) curve (light blue line); b) LAI data series for the same HMZ obtained with the SNAP toolbox: red dots represent the original values, while the blue line shows the cleaned and gap-filled LAI series.

2016–2021. Simulations were performed for each irrigation sector, keeping the same fixed irrigation dates used in the actual farm management, while optimising the water depth as explained for the pilot pivot.

An example of the simulation results obtained for an irrigation sector is shown in Fig. 13. The two panels represent the simulations carried out for the two soil types (coarse, in the upper panel, and fine, in the lower panel) belonging to the same HMZ in the 2018 agricultural season. In both panels, the red line represents the simulated water content in the root zone, while the green, yellow and orange dotted lines represent the water content at field capacity, at the irrigation threshold indicated by Allen et al., 1998 (i.e., when RAW is depleted) and at the wilting point, respectively. The simulated irrigations for both soil types are the same, as the water depth provided at each irrigation turn was calculated as the highest of the two values calculated for the two HSZs. As a benchmark, the actual irrigation provided by the farm irrigation management is also shown in the figure.

The simulation results are presented in two ways: 1) the average, maximum and minimum seasonal irrigation depths for each sprinkler system were calculated for all seasons in which the system was cropped with maize; 2) the total irrigation demand was calculated for each simulation year for the whole farm (i.e., all sprinkler systems

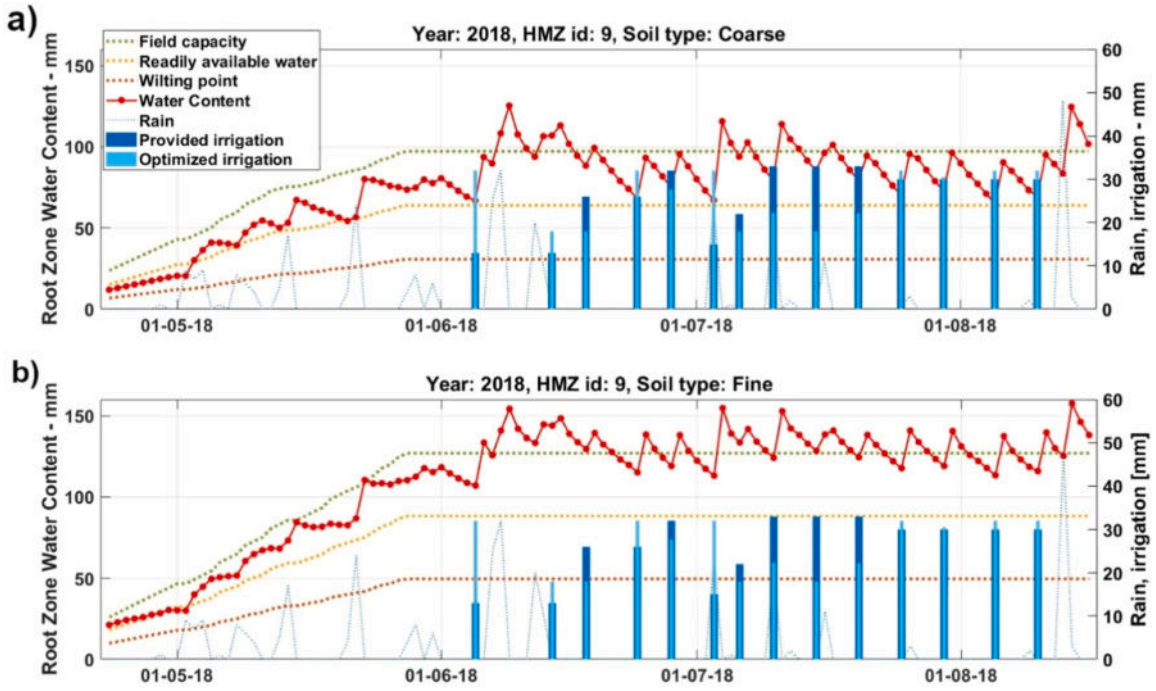

Fig. 13. Example of model simulation results for two HSZs belonging to the same HMZ: a) coarse soil; b) fine soil. In both panels the red line represents the total water content in the rooted zone, while the green, yellow and orange dotted lines represent the water content at the field capacity, at the FAO irrigation threshold and at the wilting point, respectively.

aggregated).

The results confirm the potential of variable rate irrigation (VR) to achieve significant water savings in maize production. At the level of individual sprinkler systems (see Table 4 and Fig. 1b for irrigation system codes), optimized VR irrigation led to reductions in irrigation between 12 % and 28 %. At the farm scale, total irrigation savings ranged from 6 % to 27 %, averaging 19 % over the six-year period (see Table 5 for irrigation volumes in m^3). Higher savings were observed for sprinkler systems with finer soils (systems 1, 5 and 6, which have 63 %, 54 % and 78 % of the area covered by fine soils, respectively), whereas lower savings were found for systems where maize was present in wetter years, such as 2018 (sprinkler systems 3 and 7), due to rainfall events reducting the need for farmer-managed irrigation.

These results are generally consistent with findings from previous field studies. For example, Yari et al., 2017 reported up to 34 % irrigation reduction for maize under center pivots in Alberta, Canada, without yield loss; Sui et al. (2015) reported 21 % water savings for maize in Mississippi using a center-pivot system with five zone-control units, and O'Shaughnessy and Evett, 2010 observed 15–20 % savings using VR irrigation on maize supported by soil sensors and infrared thermometers for real-time feedback, all without reducing yields. Barker et al., 2019 documented water savings in the 6–20 % range using VR irrigation approaches guided by soil moisture sensors or remote sensing, confirming the effectiveness of VR irrigation in heterogeneous soils. Compared to these studies, our results fall within the lower–mid range of reported water savings. This is likely due to the wetter conditions in some study years limiting the potential for reducing irrigation, and to the irrigation constraints maintained in the simulations. Importantly, our approach combines real-time soil moisture monitoring with short-term weather forecasts, enabling a more dynamic adjustment of irrigation volumes than what is typically reported in other field experiments.

As with the pilot pivot, energy savings correspond to water savings, since energy is required to pump water from the wells and move the sprinklers. Therefore, the time savings achieved by adopting an optimised VR irrigation approach also translate into energy savings. It can be observed that water savings are lower in the rainiest summers (e.g., 2018), while higher savings are found in the driest summers (e.g., 2019, followed by 2021 and 2016). This result is probably due to the farm irrigation manager's perception of an increased need to irrigate crops in

Table 4
Current and simulated seasonal irrigation amounts for the seven sprinkler systems (mm). Mean, minimum and maximum values calculated for the years in which maize was grown in each system are shown (systems 3–7: 2016–2018–2020; other systems: 2017–2019–2021). Sprinkler systems codes are shown in Fig. 16.

Irrigation system	Current irrigation (mm) mean (min, max)	Optimized irrigation VR (mm) mean (min, max)	Variation VR %
1	453 (410,478)	351 (281,392)	-23
2	500 (479,527)	399 (373,418)	-20
3	460 (396,501)	374 (359,401)	-19
4	500 (479,527)	395 (371,410)	-21
5	509 (466,535)	364 (324,386)	-28
6	511 (493,535)	376 (350,404)	-26
7	421 (357,456)	370 (345,404)	-12

Table 5
Current and simulated seasonal irrigation amounts at farm level. Variations are shown in terms of irrigation volumes (m3) and percentages (%).

Year	Current irrigation (m^3)	Simulated irrigation (m^3)	Variation (m^3)	Variation (%)
2016	437,251	341,382	-95,869	-22
2017	617,352	493,007	-124,345	-20
2018	352,183	331,245	-20,938	-6
2019	590,065	428,423	-161,642	-27
2020	447,974	379,966	- 68,007	-15
2021	636,420	498,033	- 138,387	-22
Average 2016-2021				**-19**

seasons with low rainfall. This makes the modelling approach presented in this paper particularly interesting, as it is based on an accurate estimate of the real need for irrigation that takes short-term weather forecasts into account.

4. Conclusions

The Precision Irrigation (PI) management in the pilot centre pivot (15 ha) resulted in an average water saving of about 20 % compared to the "as usual" irrigation management applied in the farm (16 % and 24 % for the coarse and fine sectors, respectively) in the agricultural season 2021. This value was achieved by respecting some constraints imposed by the tenant, the absence of which would certainly have increased it. As the reduction in water consumption leads to a corresponding reduction in irrigation time, the estimated energy saving (for groundwater pumping and pivot handling) was equal to the water saving (i.e., 20 %). Variable rate yield maps showed that there were no differences in yield between the variable rate and control sectors, but grain moisture was slightly lower in the sectors where the PI approach was applied, resulting in further energy savings during grain drying. Although the model calibration was limited to a part of the cropping season 2021 and a subset of soil hydraulic parameters, the results highlight the potential of the PI approach, which is of particular interest because it relies on accurate estimates of irrigation demand, which are calculated using short-term weather forecasts. At the farm level (300 ha), the simulation of the PI approach over the period 2016–2021 resulted in water and energy savings between 12 % and 28 % for the single sprinkler system, with an average of 19 % at the farm level. Again, the constraints imposed by the farm tenant were maintained and reduced the potential gain. Estimating phenometrics and crop parameters from Sentinel-2 time series was crucial for applying the developed PI method at farm scale. Water savings were found to be lower during the wettest summers (e.g., 2018) and higher during the driest (2019, 2021 and 2016), confirming that the PI approach is effective in saving water, even and especially in the most critical years.

CRediT authorship contribution statement

Alberto Crema: Writing – review & editing, Investigation, Data curation. **Mirco Boschetti:** Writing – review & editing, Supervision, Investigation, Formal analysis. **Arianna Facchi:** Writing – review & editing, Supervision, Project administration, Investigation, Funding acquisition, Conceptualization. **Alice Mayer:** Writing – original draft, Visualization, Software, Methodology, Formal analysis, Data curation. **Bianca Ortuani:** Writing – original draft, Methodology, Investigation, Formal analysis, Conceptualization.

Declaration of Competing Interest

The authors declare that they have no known competing financial interests or personal relationships that could have appeared to influence the work reported in this paper.

Acknowledgements

We wish to thank Regione Lombardia for funding the SOS-AP project (EU-RDP 2014 – 2020, grant 201901310292), in the context of which this research was developed, and "La Canova" farm (http://lacanovasrl.it/) for hosting the experimental activities.

Data availability

Data will be made available on request.

References

Abd El-Wahed, M.H., Ali, E.A., 2013. Effect of irrigation systems, amounts of irrigation water and mulching on corn yield, water use efficiency and net profit. Agric. Water Manag 120, 64–71. https://doi.org/10.1016/j.agwat.2012.06.017.

Abioye, E.A., Abidin, M.S.Z., Mahmud, M.S.A., Buyamin, S., Ishak, M.H.I., Rahman, M.K. I.A., Otuoze, A.O., Onotu, P., Ramli, M.S.A., 2020. A review on monitoring and advanced control strategies for precision irrigation. Comput. Electron. Agric. 173, 105441. https://doi.org/10.1016/j.compag.2020.105441.

Adeyemi, O., Grove, I., Peets, S., Norton, T., 2017. Advanced monitoring and management systems for improving sustainability in precision irrigation. Sustainability 9, 353. https://doi.org/10.3390/su9030353.

Agyeman, B.T., Naouri, M., Appels, W., Liu, J., 2023. Irrigation management zone delineation and optimal irrigation scheduling for center pivot irrigation systems. IFACPap. 56, 9906–9911. https://doi.org/10.1016/j.ifacol.2023.10.674.

Ahmed, Z., Gui, D., Murtaza, G., Yunfei, L., Ali, S., 2023. An overview of smart irrigation management for improving water productivity under climate change in drylands. Agronomy 13, 2113. https://doi.org/10.3390/agronomy13082113.

Ali, A., Martelli, R., Scudiero, E., Lupia, F., Falsone, G., Rondelli, V., Barbanti, L., 2023. Soil and climate factors drive spatio-temporal variability of arable crop yields under uniform management in Northern Italy. Arch. Agron. Soil Sci. 69, 75–89. https://doi.org/10.1080/03650340.2021.1958320.

Ali, A., Rondelli, V., Martelli, R., Falsone, G., Lupia, F., Barbanti, L., 2022. Management zones delineation through clustering techniques based on soils traits, NDVI data, and multiple year crop yields. Agriculture 12, 231. https://doi.org/10.3390/agriculture12020231.

Allen, R.G., Pereira, L.S., Raes, D., Smith, M., 1998. Crop evapotranspiration: guidelines for computing crop water requirements, FAO irrigation and drainage paper. Food and Agriculture Organization of the United Nations, Rome.

Bantchina, B.B., Gündoğdu, K.S., Arslan, S., Ulusoy, Y., Tekin, Y., Pantazi, X.E., Dolaptsis, K., Paraskevas, C., Tziotzios, G., Qaswar, M., Mouazen, A.M., 2024. Spatiotemporal modeling of soil water dynamics for site-specific variable rate irrigation in maize. Soil Syst. 8, 19. https://doi.org/10.3390/soilsystems8010019.

Banton, O., Cimon, M. -A., Seguin, M. -K., 1997. Mapping field-scale physical properties of soil with electrical resistivity. Soil Sci. Soc. Am. J. 61, 1010–1017. https://doi.org/10.2136/sssaj1997.03615995006100040003x.

Barker, J.B., Bhatti, S., Heeren, D.M., Neale, C.M.U., Rudnick, D.R., 2019. Variable rate irrigation of maize and soybean in West-Central Nebraska under full and deficit irrigation. Front. Big Data 2, 34. https://doi.org/10.3389/fdata.2019.00034.

Bonfante, A., Monaco, E., Alfieri, S.M., De Lorenzi, F., Manna, P., Basile, A., Bouma, J., 2015. Climate change effects on the suitability of an agricultural area to maize cultivation. Adv. Agron. 33–69. https://doi.org/10.1016/bs.agron.2015.05.001.

Bonfante, A., Monaco, E., Manna, P., De Mascellis, R., Basile, A., Buonanno, M., Cantilena, G., Esposito, A., Tedeschi, A., De Michele, C., Belfiore, O., Catapano, I., Ludeno, G., Salinas, K., Brook, A., 2019. LCIS DSS—An irrigation supporting system for water use efficiency improvement in precision agriculture: A maize case study. Agric. Syst. 176, 102646. https://doi.org/10.1016/j.agsy.2019.102646.

Breunig, F.M., Galvão, L.S., Dalagnol, R., Dauve, C.E., Parraga, A., Santi, A.L., Della Flora, D.P., Chen, S., 2020. Delineation of management zones in agricultural fields using cover–crop biomass estimates from PlanetScope data. Int. J. Appl. Earth Obs. Geoinf. 85, 102004. https://doi.org/10.1016/j.jag.2019.102004.

Ciavatta, C., Vianello, G., 1989. Bilancio idrico dei suoli: applicazioni tassonomiche, climatiche e cartografiche. CLUEB, Bologna.

Cohen, Y., Alchanatis, V., Saranga, Y., Rosenberg, O., Sela, E., Bosak, A., 2017. Mapping water status based on aerial thermal imagery: comparison of methodologies for upscaling from a single leaf to commercial fields. Precis. Agric. 18, 801–822. https://doi.org/10.1007/s11119-016-9484-3.

Corwin, D.L., Lesch, S.M., 2003. Application of Soil Electrical Conductivity to Precision Agriculture: Theory, Principles, and Guidelines. Agron. J. 95, 455–471. https://doi.org/10.2134/agronj2003.4550.

Corwin, D.L., Plant, R.E., 2005. Applications of apparent soil electrical conductivity in precision agriculture. Comput. Electron. Agric. 46, 1–10. https://doi.org/10.1016/j.compag.2004.10.004.

Corwin, D.L., Scudiero, E., 2020. Field-scale apparent soil electrical conductivity. Soil Sci. Soc. Am. J. 84, 1405–1441. https://doi.org/10.1002/saj2.20153.

Crema, A., Boschetti, M., Nutini, F., Cillis, D., Casa, R., 2020. Influence of Soil Properties on Maize and Wheat Nitrogen Status Assessment from Sentinel-2 Data. Remote Sens 12, 2175. https://doi.org/10.3390/rs12142175.

D.d.s 4346, 2018. Approvazione della «Metodologia di stima dei volumi idrici ad uso irriguo, in attuazione della d.g.r. n. 6035/2016». Available at: ⟨https://www.regione.lombardia.it/wps/wcm/connect/8f7c5df8-e897-47b7-b5fd-62c541b9bc67/decreto-4346-2018-metodologia-stima-volumi-idrici-uso-irriguo.pdf?MOD=AJPERES&CACHEID=8f7c5df8-e897-47b7-b5fd-62c541b9bc67⟩. [Accessed: 13 Apr 2025].

Dahal, S., Phillippi, E., Longchamps, L., Khosla, R., Andales, A., 2020. Variable Rate Nitrogen and Water Management for Irrigated Maize in the Western US. Agronomy 10, 1533. https://doi.org/10.3390/agronomy10101533.

De Peppo, M., Ragaglini, G., Carmagnola, F., Corti, M., Mayer, A., Facchi, A., Ortuani, B., Bechini, L., Nutini, F., Crema, A., Boschetti, M., 2022. Coherence Assessment Between Satellite-based phenometrics And ARMOSA Crop Model Simulations For Maize Phenology Estimation, in: Proceedings of the 51st National Conference of the Italian Society for Agronomy (Dalla Marta A., Maucieri C., Ventrella D., Eds.). Presented at the Agriculture and food availability in 2050, Padova, Italy, pp. 163–164.

Dehghanisanij, H., Kouhi, N., 2020. Interactive effects of nitrogen and drip irrigation rates on root development of corn (Zea mays L.) and residual soil moisture. Gesund Pflanz. 72, 335–349. https://doi.org/10.1007/s10343-020-00516-4.
ERSAF, (n.d.). Banca Dati Suoli LOSAN. [Online] Available at: ⟨https://losan.ersaflombardia.it/⟩ [Accessed: 21 Oct 2025].
Evans, R.G., LaRue, J., Stone, K.C., King, B.A., 2013. Adoption of site-specific variable rate sprinkler irrigation systems. Irrig. Sci. 31, 871–887. https://doi.org/10.1007/s00271-012-0365-x.
Facchi, A., Gharsallah, O., Corbari, C., Masseroni, D., Mancini, M., Gandolfi, C., 2013. Determination of maize crop coefficients in humid climate regime using the eddy covariance technique. Agric. Water Manag 130, 131–141. https://doi.org/10.1016/j.agwat.2013.08.014.
FAO, n.d. FAOSTAT Crops and livestock products database [Online] Available at: ⟨https://www.fao.org/faostat/en/#data/QCL⟩ [Accessed: 18 Dec 2025].
Feddes, R.A., Kowalik, Piotr, J., Zaradny, Henryk, Feddes, R.A., Kowalik, P.J., Zaradny, H., 1978. Simulation of field water use and crop yield, Simulation monographs. Centre for Agricultural Publishing and Documentation, Wageningen.
Feki, M., Ravazzani, G., Ceppi, A., Mancini, M., 2018. Influence of soil hydraulic variability on soil moisture simulations and irrigation scheduling in a maize field. Agric. Water Manag 202, 183–194. https://doi.org/10.1016/j.agwat.2018.02.024.
Fitzgerald, G.J., Lesch, S.M., Barnes, E.M., Luckett, W.E., 2006. Directed sampling using remote sensing with a response surface sampling design for site-specific agriculture. Comput. Electron. Agric. 53, 98–112. https://doi.org/10.1016/j.compag.2006.04.003.
Fleming, K.L., Westfall, D.G., Wiens, D.W., Brodahl, M.C., 2000. Evaluating Farmer Defined Management Zone Maps for Variable Rate Fertilizer Application. Precis. Agric. 2, 201–215. https://doi.org/10.1023/A:1011481832064.
Flint, E.A., Hopkins, B.G., Svedin, J.D., Kerry, R., Heaton, M.J., Jensen, R.R., Campbell, C.S., Yost, M.A., Hansen, N.C., 2023. Irrigation Zone Delineation and Management with a Field-Scale Variable Rate Irrigation System in Winter Wheat. Agronomy 13, 1125. https://doi.org/10.3390/agronomy13041125.
Fontanet, M., Scudiero, E., Skaggs, T.H., Fernàndez-Garcia, D., Ferrer, F., Rodrigo, G., Bellvert, J., 2020. Dynamic Management Zones for Irrigation Scheduling. Agric. Water Manag 238, 106207. https://doi.org/10.1016/j.agwat.2020.106207.
Fridgen, J.J., Kitchen, N.R., Sudduth, K.A., Drummond, S.T., Wiebold, W.J., Fraisse, C. W., 2004. Management Zone Analyst (MZA): Software for Subfield Management Zone Delineation. Agron. J. 96, 100–108. https://doi.org/10.2134/agronj2004.1000.
Gao, Y., Duan, A., Qiu, X., Liu, Z., Sun, J., Zhang, J., Wang, H., 2010. Distribution of roots and root length density in a maize/soybean strip intercropping system. Agric. Water Manag 98, 199–212. https://doi.org/10.1016/j.agwat.2010.08.021.
Georgi, C., Spengler, D., Itzerott, S., Kleinschmit, B., 2018. Automatic delineation algorithm for site-specific management zones based on satellite remote sensing data. Precis. Agric. 19, 684–707. https://doi.org/10.1007/s11119-017-9549-y.
Greaves, G., Wang, Y.-M., 2016. Assessment of FAO AquaCrop Model for Simulating Maize Growth and Productivity under Deficit Irrigation in a Tropical Environment. Water 8, 557. https://doi.org/10.3390/w8120557.
Gupta, S., Kumar, M., Priyadarshini, R., 2019. Electrical Conductivity Sensing for Precision Agriculture: A Review. In: Yadav, N., Yadav, A., Bansal, J.C., Deep, K., Kim, J.H. (Eds.), Harmony Search and Nature Inspired Optimization Algorithms, Advances in Intelligent Systems and Computing. Springer Singapore, Singapore, pp. 647–659. https://doi.org/10.1007/978-981-13-0761-4_62.
Haghverdi, A., Leib, B.G., Washington-Allen, R.A., Ayers, P.D., Buschermohle, M.J., 2015. Perspectives on delineating management zones for variable rate irrigation. Comput. Electron. Agric. 117, 154–167. https://doi.org/10.1016/j.compag.2015.06.019.
Hedley, C.B., Yule, I.J., 2009a. A method for spatial prediction of daily soil water status for precise irrigation scheduling. Agric. Water Manag 96, 1737–1745. https://doi.org/10.1016/j.agwat.2009.07.009.
Hedley, C.B., Yule, I.J., 2009b. Soil water status mapping and two variable-rate irrigation scenarios. Precis. Agric. 10, 342–355. https://doi.org/10.1007/s11119-009-9119-z.
IMA (Italian Ministry of Agriculture), 1999. Decreto Ministeriale 13/09/1999, n. 185: Approvazione dei Metodi ufficiali di analisi chimica del suolo. Gazzetta Ufficiale, Suppl. Ord. n. 248, 21 Oct 1999. Available at: ⟨https://www.gazzettaufficiale.it/eli/id/1999/10/21/099A8497/sg⟩.
ISTAT, n.d. Agricultural census data. [Online] Available at: ⟨https://esploradati.istat.it/databrowser/#/it/censimentoagricoltura⟩ [Accessed: 18 Dec 2025].
Jiang, J., Feng, S., Ma, J., Huo, Z., Zhang, C., 2016. Irrigation management for spring maize grown on saline soil based on SWAP model. Field Crops Res 196, 85–97. https://doi.org/10.1016/j.fcr.2016.06.011.
Kottek, M., Grieser, J., Beck, C., Rudolf, B., Rubel, F., 2006. World Map of the Köppen-Geiger climate classification updated. Meteorol. Z. 15, 259–263. https://doi.org/10.1127/0941-2948/2006/0130.
Kroes, J.G., Van Dam, J.C., Bartholomeus, R.P., Groenendijk, P., Heinen, M., Hendriks, R. F.A., Mulder, H.M., Supit, I., Van Walsum, P.E.V., 2017. SWAP version 4. Wageningen Environmental Research, Wageningen. https://doi.org/10.18174/416321.
Li, P., Ren, L., 2019. Evaluating the effects of limited irrigation on crop water productivity and reducing deep groundwater exploitation in the North China Plain using an agro-hydrological model: I. Parameter sensitivity analysis, calibration and model validation. J. Hydrol. 574, 497–516. https://doi.org/10.1016/j.jhydrol.2019.04.053.
Liakos, V., Porter, W., Liang, X., Tucker, M.A., McLendon, A., Vellidis, G., 2017. Dynamic Variable Rate Irrigation – A Tool for Greatly Improving Water Use Efficiency. Adv. Anim. Biosci. 8, 557–563. https://doi.org/10.1017/S2040470017000711.
Liu, H., Whiting, M.L., Ustin, S.L., Zarco-Tejada, P.J., Huffman, T., Zhang, X., 2018. Maximizing the relationship of yield to site-specific management zones with object-oriented segmentation of hyperspectral images. Precis. Agric. 19, 348–364. https://doi.org/10.1007/s11119-017-9521-x.
Mahgoub, N.A., Ibrahim, A.M., Ali, O.M., 2017. Effect of different irrigation systems on root growth of maize and cowpea plants in sandy soil. Eurasia J. Soil Sci. 6, 374–379. https://doi.org/10.18393/ejss.319952.
Masseroni, D., Gangi, F., Galli, A., Ceriani, R., De Gaetani, C., Gandolfi, C., 2022. Behind the efficiency of border irrigation: Lesson learned in Northern Italy. Agric. Water Manag 269, 107717. https://doi.org/10.1016/j.agwat.2022.107717.
Matese, A., Di Gennaro, S.F., 2015. Technology in precision viticulture: a state of the art review. Int. J. Wine Res 69. https://doi.org/10.2147/IJWR.S69405.
Monaco, E., Bonfante, A., Alfieri, S.M., Basile, A., Menenti, M., De Lorenzi, F., 2014. Climate change, effective water use for irrigation and adaptability of maize: A case study in southern Italy. Biosyst. Eng. 128, 82–99. https://doi.org/10.1016/j.biosystemseng.2014.09.001.
Montanari, A., Nguyen, H., Rubinetti, S., Ceola, S., Galelli, S., Rubino, A., Zanchettin, D., 2023. Why the 2022 Po River drought is the worst in the past two centuries. Sci. Adv. 9, eadg8304. https://doi.org/10.1126/sciadv.adg8304.
Neupane, J., Guo, W., 2019. Agronomic Basis and Strategies for Precision Water Management: A Review. Agronomy 9, 87. https://doi.org/10.3390/agronomy9020087.
Nutini, F., Confalonieri, R., Crema, A., Movedi, E., Paleari, L., Stavrakoudis, D., Boschetti, M., 2018. An operational workflow to assess rice nutritional status based on satellite imagery and smartphone apps. Comput. Electron. Agric. 154, 80–92. https://doi.org/10.1016/j.compag.2018.08.008.
O'Shaughnessy, S.A., Evett, S.R., 2010. Developing Wireless Sensor Networks for Monitoring Crop Canopy Temperature Using a Moving Sprinkler System as a Platform. Appl. Eng. Agric. 26, 331–341. https://doi.org/10.13031/2013.29534.
Ortuani, Facchi, Mayer, Bianchi, Bianchi, Brancadoro, 2019. Assessing the Effectiveness of Variable-Rate Drip Irrigation on Water Use Efficiency in a Vineyard in Northern Italy. Water 11, 1964. https://doi.org/10.3390/w11101964.
Pampana, S., Ercoli, L., Masoni, A., Arduini, I., 2009. Remobilization of Dry Matter and Nitrogen in Maize as Affected by Hybrid Maturity Class. Ital. J. Agron. 4, 39. https://doi.org/10.4081/ija.2009.2.39.
Pan, Y., Yuan, C., Jing, S., 2020. Simulation and optimization of irrigation schedule for summer maize based on SWAP model in saline region. Int. J. Agric. Biol. Eng. 13, 117–122. https://doi.org/10.25165/j.ijabe.20201303.5218.
Pellegrini, S., Vignozzi, N., Costantini, E.A.C., L"Abate, G., 2007. A new pedotransfer function for estimating soil bulk density. Presented at the 5th International Congress of the ESSC – Palermo, June, 25-30 2007. Available at: ⟨https://www.academia.edu/39573231/A_new_pedotransfer_function_for_estimating_soil_bulk_density⟩. [Accessed: 14 Apr 2025].
Perego, A., Giussani, A., Sanna, M., Fumagalli, M., Carozzi, M., Brenna, S., Acutis, M., 2013. The ARMOSA simulation crop model: overall features, calibration and validation results. Ital. J. Agron. 18 (3), 23–38.
Ranghetti, L., 2022. sen2rts: Version 0.4.1. https://doi.org/10.5281/ZENODO.4682829.
Ranghetti, L., Boschetti, M., Nutini, F., Busetto, L., 2020. sen2r": An R toolbox for automatically downloading and preprocessing Sentinel-2 satellite data. Comput. Geosci. 139, 104473. https://doi.org/10.1016/j.cageo.2020.104473.
Ranghetti, L., Nutini, F., Cillis, D., Boschetti, M., 2021. A Reproducible Workflow to Derive Crop Phenology and Agro-Practice Information from Sentinel-2 Time Series: a Case Study for Sardinia Cropping Systems, in: X AIT International Conference - Italian Society of Remote Sensing, Cagliari, 13-15/09/2021. AIT Series: Trends in Earth Observation. Associazione Italiana di Telerilevamento (AIT), pp. 133–136. https://doi.org/10.978.88944687/00.
Reyes, J., Wendroth, O., Matocha, C., Zhu, J., 2019. Delineating site-specific management zones and evaluating soil water temporal dynamics in a farmer's field in Kentucky. Vadose zone J. 18, 1–19. https://doi.org/10.2136/vzj2018.07.0143.
Schenatto, K., Souza, E.G., Bazzi, C.L., Beneduzzi, H.M., 2015. Management Zones with NDVI Data through Corn and Soybean Yield. Presented at the First Conference on Proximal Sensing Supporting Precision Agriculture, Turin, Italy. https://doi.org/10.3997/2214-4609.201413856.
Scudiero, E., Lesch, S.M., Corwin, D.L., 2016. Validation of sensor-directed spatial simulated annealing soil sampling strategy. J. Env Qual. 45, 1226–1233. https://doi.org/10.2134/jeq2015.09.0458.
Scudiero, E., Teatini, P., Manoli, G., Braga, F., Skaggs, T., Morari, F., 2018. Workflow to establish time-specific zones in precision agriculture by spatiotemporal integration of plant and soil sensing data. Agronomy 8, 253. https://doi.org/10.3390/agronomy8110253.
Serrano, J., Shahidian, S., Marques Da Silva, J., Paixão, L., Carreira, E., Pereira, A., Carvalho, M., 2020. Climate changes challenges to the management of Mediterranean Montado ecosystem: perspectives for use of precision agriculture technologies. Agronomy 10, 218. https://doi.org/10.3390/agronomy10020218.
Singh, B.R., Singh, D.P., 1995. Agronomic and physiological responses of sorghum, maize and pearl millet to irrigation. Field Crops Res 42, 57–67. https://doi.org/10.1016/0378-4290(95)00025-L.
Singh, R., van Dam, J.C., Feddes, R.A., 2006. Water productivity analysis of irrigated crops in Sirsa district, India. Agric. Water Manag 82, 253–278. https://doi.org/10.1016/j.agwat.2005.07.027.
Speranza, E.A., Naime, J.D.M., Vaz, C.M.P., Santos, J.C.F.D., Inamasu, R.Y., Lopes, I.D.O. N., Queirós, L.R., Rabelo, L.M., Jorge, L.A.D.C., Chagas, S.D., Schelp, M.X., Vecchi, L., 2023. Delineating Management Zones with Different Yield Potentials in Soybean–Corn and Soybean–Cotton Production Systems. AgriEngineering 5, 1481–1497. https://doi.org/10.3390/agriengineering5030092.

Steduto, P., Hsiao, T.C., Fereres, E., Raes, Dirk, 2012. Crop yield response to water, FAO Irrigation and Drainage Paper 66. Food and Agriculture Organizations of the United Nations, Roma.

Sui, R., Fisher, D.K., Reddy, K.N., 2015. Yield Response to Variable Rate Irrigation in Corn. JAS 7, p11. https://doi.org/10.5539/jas.v7n11p11.

T.A.S. Team, 2021. Sentinel-2 Products Specification Document, v. 14.9 Available at: ⟨https://sentinel.esa.int/documents/247904/685211/S2-PDGS-TAS-DI-PSD-V14.9.pdf⟩. [Accessed: 14 Apr 2025].

Termin, D., Linker, R., Baram, S., Raveh, E., Ohana-Levi, N., Paz-Kagan, T., 2023. Dynamic delineation of management zones for site-specific nitrogen fertilization in a citrus orchard. Precis. Agric. 24, 1570–1592. https://doi.org/10.1007/s11119-023-10008-w.

Thorp, K.R., 2020. Long-term simulations of site-specific irrigation management for Arizona cotton production. Irrig. Sci. 38, 49–64. https://doi.org/10.1007/s00271-019-00650-6.

Toreti, A., Bassu, S., Asseng, S., Zampieri, M., Ceglar, A., Royo, C., 2022. Climate service driven adaptation may alleviate the impacts of climate change in agriculture. Commun. Biol. 5, 1235. https://doi.org/10.1038/s42003-022-04189-9.

Xue, C., Ghirardelli, A., Chen, J., Tarolli, P., 2024. Investigating agricultural drought in Northern Italy through explainable Machine Learning: Insights from the 2022 drought. Comput. Electron. Agric. 227, 109572. https://doi.org/10.1016/j.compag.2024.109572.

Yari, A., Madramootoo, C.A., Woods, S.A., Adamchuk, V.I., 2017. Performance evaluation of constant versus variable rate irrigation. Irrig. Drain. 66, 501–509. https://doi.org/10.1002/ird.2131.

Yuan, C., Feng, S., Huo, Z., Ji, Q., 2019. Simulation of saline water irrigation for seed maize in arid Northwest China Based on SWAP model. Sustainability 11, 4264. https://doi.org/10.3390/su11164264.

Zhang, J., Guan, K., Peng, B., Jiang, C., Zhou, W., Yang, Y., Pan, M., Franz, T.E., Heeren, D.M., Rudnick, D.R., Abimbola, O., Kimm, H., Caylor, K., Good, S., Khanna, M., Gates, J., Cai, Y., 2021. Challenges and opportunities in precision irrigation decision-support systems for center pivots. Environ. Res. Lett. 16, 053003. https://doi.org/10.1088/1748-9326/abe436.

Zhang, Y., Schaap, M.G., 2017. Weighted recalibration of the Rosetta pedotransfer model with improved estimates of hydraulic parameter distributions and summary statistics (Rosetta3). J. Hydrol. 547, 39–53. https://doi.org/10.1016/j.jhydrol.2017.01.004.